Cell-cycle quiescence maintains *C. elegans* germline stem cells independent of GLP-1/Notch

Hannah S. Seidel[1,2] and Judith Kimble[1,3]

[1]Department of Biochemistry, University of Wisconsin-Madison, [2]Ellison Medical Foundation Fellow of the Life Science Research Foundation, [3]Howard Hughes Medical Institute

Abstract

Many types of adult stem cells exist in a state of cell-cycle quiescence, yet it has remained unclear whether quiescence plays a role in maintaining the stem cell fate. Here we establish the adult germline of *C. elegans* as model for facultative stem cell quiescence. We find that mitotically dividing germ cells—including germline stem cells—become quiescent in the absence of food. This quiescence is characterized by a slowing of S phase, a block to M-phase entry, and the ability to re-enter M phase rapidly in response to re-feeding. Further, we demonstrate that cell-cycle quiescence alters the genetic requirements for stem cell maintenance: The signaling pathway required for stem cell maintenance under fed conditions—GLP-1/Notch signaling—becomes dispensable under conditions of quiescence. Thus, cell-cycle quiescence can itself maintain stem cells, independent of the signaling pathway otherwise essential for such maintenance.

Introduction

Stem cells in adult tissues were once thought to exist primarily in a state of cell-cycle quiescence. Such quiescence was viewed as an inherent property of the stem cell fate and thus essential for a tissue's long-term self-renewal (Hall and Watt, 1989; Potten and Loeffler, 1990). More recently, however, it has become clear that adult stem cells are not universally quiescent but instead cycle in accordance with the needs of the tissue: Some types of stem cells proliferate continuously, whereas others switch from quiescence to rapid proliferation in response to certain stimuli (e.g. wounding or hormones) (Wabik and Jones, 2015). In mammals, for example, hematopoietic and neural stem cells reversibly switch between quiescence and active proliferation in response to tissue injury (Doetsch et al., 1999; Harrison and Lerner, 1991; Lugert et al., 2010), and mammary stem cells expand transiently during pregnancy and the estrus cycle (Asselin-Labat et al., 2010; Joshi et al., 2010). Though periods of sustained stem cell proliferation enable rapid tissue growth or turnover, they challenge the view of quiescence as a prerequisite for the stem cell fate. Thus, a long-standing question has remained unanswered: Does cell-cycle quiescence play a role in stem cell maintenance?

Understanding the relationship between cell-cycle quiescence and stem cell maintenance has been difficult because tractable models of facultative stem cell quiescence have been lacking. Perturbations affecting the cell cycle can in some cases impact stem cell maintenance (Orford and Scadden, 2008; Pietras et al., 2011; Yilmaz et al., 2012), but whether quiescence can maintain stem cells independent of the signals otherwise required for their maintenance has been untested. Such a test requires a system in which cell-cycle quiescence can be readily induced, and in which the signals otherwise required for stem cell maintenance can be readily removed. In this study, we establish the adult germline of *Caenorhabditis elegans* as a model fitting these criteria. We describe a previously uncharacterized state of cell-cycle quiescence among adult germline stem cells, emerging under conditions of starvation. We then test whether this quiescence can maintain stem cells, independent of the signal otherwise required for their maintenance.

The adult germline of *C. elegans* presents a tractable model for studying stem cell behavior because of its simple, linear organization (Figure 1A). Mitotically dividing germ cells—including germline stem cells—reside in the distal region of the gonad (the 'progenitor zone'). Differentiating germ cells, in meiotic prophase, are located more proximally. (Here we

use the term ‘progenitor zone’ rather than the earlier terms ‘mitotic zone’ or ‘proliferative zone’ to reflect the facultative nature of germ cell divisions.) The progenitor zone has been studied under fed conditions and is composed of a distal pool of germline stem cells and a more proximal pool of cells that have begun to differentiate (Cinquin et al., 2010). This proximal pool comprises cells dividing mitotically, as well as cells completing their final passage through interphase in preparation for entry into the meiotic cell cycle. We collectively refer to these cells as ‘transient progenitors’, to reflect their continued mitotic divisions and transitional state (Figure 1A). Under fed conditions, cells throughout the progenitor zone cycle asynchronously and continuously (Crittenden et al., 2006; Fox et al., 2011; Jaramillo-Lambert et al., 2007; Morgan et al., 2010), with transient progenitors undergoing one or two rounds of division as they pass through the proximal progenitor zone (Fox and Schedl, 2015).

Prior to this work, germ cell proliferation in *C. elegans* adults had not been examined in detail under food-limited conditions. However, the effects of such conditions have been examined during larval development in *C. elegans,* as well as in adult *Drosophila*, and in both contexts, germ cells respond robustly to nutritional cues. In *Drosophila*, nutrient limitation or changes in nutrient-sensing pathways slows germline cell proliferation, reduces germline stem cell number, or both (Armstrong et al., 2014; Drummond-Barbosa and Spradling, 2001; Hsu et al., 2008; LaFever et al., 2010; McLeod et al., 2010; Roth et al., 2012; Sheng and Matunis, 2011). These effects are mediated in part by changes in the somatic gonad (Yang and Yamashita, 2015), including changes in the size of the somatic niche supporting germline stem cells (Bonfini et al., 2015; Hsu and Drummond-Barbosa, 2011). In *C. elegans*, primordial germ cells are born in the early embryo and arrest in the G2 phase of the cell cycle until newly hatched larvae begin to feed (Butuci et al., 2015; Fukuyama et al., 2006; Fukuyama et al., 2012). This response to feeding has been hypothesized to involve food-related signals traveling through soma-to-germline gap junctions, which are required early in larval development for germ cell proliferation and survival (Starich et al., 2014). Later in development, germ cells stop dividing if animals enter the non-feeding dauer larval stage (Narbonne and Roy, 2006). Even in non-dauer larvae, germ cells proliferate less when food is scarce, an effect mediated in part by communication between food-sensing neurons and the somatic gonad (Dalfo et al., 2012; Korta et al., 2012). In adult *C. elegans*, decreased food intake slows mitotic and meiotic progression and oogenesis (Gerhold et al., 2015; Lopez et al., 2013; Salinas et al., 2006; Seidel and Kimble,

2011), and limited observations suggest that germ cell proliferation is also reduced (Salinas et al., 2006). More strikingly, full starvation from the L4 larval stage causes dramatic germline shrinkage in adult hermaphrodites, and this shrinkage is reversible upon re-feeding (Angelo and Van Gilst, 2009; Seidel and Kimble, 2011). These observations motivated us to examine in greater detail how mitotically dividing germ cells in adult *C. elegans* respond to food removal.

Here we report that in the absence of food, mitotically dividing germ cells in adult *C. elegans* stop dividing and become quiescent. This quiescence is characterized by a dramatic slowing of S phase, cell-cycle arrest in G2, and the ability to re-enter M phase rapidly in response to re-feeding. We investigate these cell-cycle responses in wildtype animals and in germline tumors, and we test whether this cell-cycle quiescence requires factors controlling larval or behavioral responses to food. We next investigate the control of stem cell maintenance under starved conditions. We uncover a major difference in the requirement for GLP-1/Notch signaling in the maintenance of actively proliferating versus quiescent germline stem cells. This work establishes the *C. elegans* germline as model of facultative stem cell quiescence and demonstrates the utility of such a model in clarifying the role of quiescence in maintaining the stem cell state.

Results

M-phase entry in adult germ cells responds rapidly to starvation and re-feeding

To investigate how starvation affects germ cell division in adults, we removed food from early adult hermaphrodites and males and monitored the number of germ cells in M phase over the following 10.5 hours. Cells in M phase were identified by staining for phospho-histone H3 (Figure 1B), a marker of M phase (Hans and Dimitrov, 2001). Food removal caused a drop in the number of M-phase cells (Figure 2A), and this response was fast: In hermaphrodites, the number of M-phase cells per progenitor zone dropped from an average of 7.6 before food removal to 2.1 after 30 minutes without food (n = 7 replicates of 220 – 551 gonadal arms per replicate per timepoint) (Figure 2A). The number of M-phase cells continued to decline thereafter, and after 3.5 hours without food, M-phase cells were virtually absent (Figure 2A). This drop in M-phase cells did not occur in hermaphrodites fed continuously (Figure 2—figure supplement 1B,D), nor in hermaphrodites exposed to a mock starvation procedure (Figure 2—figure supplement 1C). In males, M-phase cells also disappeared rapidly in response to food removal, although the initial drop in M-phase cells was not monotonically decreasing (Figure 2B). We conclude that in adults

of both sexes, germ cells stop dividing quickly in the absence of food.

We next investigated how germ cell division responds to re-feeding. We removed food from early adult hermaphrodites and males, allowed animals to remain in starvation for 12 hours, then re-fed animals and monitored the number of M-phase cells, as above. In hermaphrodites, this treatment triggered a burst of M-phase cells 1.5 hours after the start of re-feeding (Figure 2D). Males showed a similar response to re-feeding, but the burst of M-phase cells occurred one hour earlier (Figure 2E). In both sexes, these bursts included some individual germlines having approximately twice as many M-phase cells as were observed among continuously fed animals (Figure 2—figure supplement 1E-F). These results demonstrate that in both sexes, germ cells resume mitotic division rapidly in response to re-feeding. The faster response in males is consistent with germ cells in males having a faster cell-cycle under continuously fed conditions (Morgan et al., 2010). Further, the higher maxima of M-phase cells in re-fed versus continuously fed animals is consistent with germ cells collecting at the G2-to-M transition during starvation and entering M phase semi-synchronously upon re-feeding.

Cessation of M-phase entry in response to starvation coincides with the molt into adulthood

We next extended our results to adult hermaphrodites starved from the L4 larval stage. This extension was motivated by the need to perform certain later experiments in such animals, as starvation from L4 prolongs the amount of time that adult hermaphrodites can be maintained without food (Angelo and Van Gilst, 2009; Seidel and Kimble, 2011). We removed food from mid-L4 hermaphrodites and monitored the number of cells in M phase, as above. In starved L4s, M-phase cells persisted for ~4-5 hours after food removal, with the average number of M-phase cells only moderately reduced relative to fed animals (Figure 2C). Thereafter, the number of M-phase cells declined rapidly, and after 10.5 hours without food, M-phase cells had virtually disappeared (Figure 2C). The disappearance of M-phase cells coincided with the molt into adulthood (~5-8 hours after food removal), and the coincidence of these events persisted even under conditions where the timing of this molt was changed: Hermaphrodites starved from early L4 molted into adulthood ~12-20 hours after food removal, and gonads in these animals contained, on average, 1.6 M-phase cells per progenitor zone before the molt (n = 57, gonads collected 10.5 hours post food removal) and 0.0 M-phase cells after the molt (n = 63, gonads collected 24 hours post food removal). These results demonstrate that germ cells in hermaphrodites starved from L4 do not immediately stop dividing in response to food removal,

but germ cell division eventually ceases, at or near the molt into adulthood. This finding suggests that mitotically dividing germ cells in L4s are not equivalent to those in adults, a result consistent with previous studies (Crittenden et al., 2002; Dalfo et al., 2012; Gerhold et al., 2015; Michaelson et al., 2010).

Longer starvation does not delay M-phase entry upon re-feeding

In other systems, re-entry into the mitotic cell cycle following a period of quiescence occurs more slowly after longer periods of quiescence (Lum et al., 2005; Soprano, 1994). We therefore tested whether longer periods of starvation would delay mitotic re-entry upon re-feeding. We repeated the re-feeding timecourse in two types of animals having experienced longer starvation: Adult hermaphrodites starved from mid L4 for 24 hours and adult hermaphrodites starved from early L4 for 72 hours. In both types of animals, re-feeding triggered a burst of M-phase cells 1.5 hours after re-feeding (Figure 2F), similar to the re-feeding response in animals starved for only 12 hours (compare Figure 2D versus F). We conclude that the timing of M-phase entry upon re-feeding is largely unaffected by the duration of preceding starvation, at least during the first 72 hours of starvation.

During starvation, germ cells progress slowly through S phase and arrest in G2

We next examined how starvation affects progression of germ cells through G1, S phase, and G2. First, we monitored cell-cycle progression in fed animals. By labeling germlines with the thymidine analog EdU and monitoring the fraction of EdU^+ M-phase cells over time, we estimated a median cell-cycle length in fed early adult hermaphrodites of ~6.2 hours, with S phase lasting ~4.4 hours, G2 lasting ~1.3 hours, and G1 and M phase together lasting ~30 minutes (Figure 3—figure supplement 1). We also measured cell-cycle length in fed hermaphrodites aged 24-hours post mid L4 (~12-16 hours past the early adult stage). For this age group, we estimated a median cell-cycle length of ~9.8 hours, with median G1, S-phase, and G2 lengths of less than 30 minutes, ~6.8 hours, and ~2.3 hours, respectively, but with a long-tailed distribution of G2 lengths (Figure 3—figure supplement 1). Our estimates of median cell-cycle length are within the range reported by others (Crittenden et al., 2006; Fox et al., 2011; Jaramillo-Lambert et al., 2007; Morgan et al., 2010), and the long-tailed distribution of G2 lengths is consistent with estimates of maximal cell-cycle length being considerably longer than estimates of median cell-cycle length (Crittenden et al., 2006; Fox et al., 2011; Jaramillo-Lambert et al., 2007; Morgan et al., 2010).

Second, we monitored cell-cycle progression during starvation. We removed food from animals of both sexes and, after varying amounts of time, calculated the fraction of progenitor-zone cells in G1, S phase, and G2. S-phase cells were identified by EdU labeling, and G1 versus G2 cells were distinguished by nuclear size (see 'Use of nuclear size to distinguish G1 versus G2 cells' in Materials and methods and Figure 3—figure supplement 2). The following timepoints were collected: Animals starved from early adult for 3.5, 6.5, and 10.5 hours; animals starved from mid L4 for 10.5 and 24 hours; and animals starved from early L4 for 10.5, 24, 48 and 72 hours. For all three age groups and for both sexes, G1 cells disappeared following food removal, and the timing of their disappearance coincided with the disappearance of M-phase cells (Figure 3A). This result demonstrates that during starvation, G1 cells continued to initiate S phase without a pronounced delay. Our second observation was that for all age groups and sexes, the fraction of S-phase cells decreased over time during starvation, and the fraction of G2 cells increased (Figure 3A). However, S-phase and G2 fractions changed more slowly during starvation than expected from measurements of S-phase length in fed animals (Figure 3A). [For example, in hermaphrodites starved from early adult, S-phase fractions changed very little during the seven hours between timepoints 3.5 hours and 10.5 hours (Figure 3A), indicating that progression through S phase during this time period was minimal. By contrast, cells in fed adult hermaphrodites complete S phase in a median of ~4.4-6.8 hours (Figure 3—figure supplement 1).] We conclude that during starvation, germ cells do not pause in G1 and instead continue through S phase and arrest in G2. However, S-phase progression occurs much more slowly than under fed conditions.

Re-feeding restores the rate of progression through S phase and G2

We next examined the effect of re-feeding on cell-cycle progression through S phase and G2. We re-fed starved animals and determined the length of time until all germ cells entered M phase. This analysis is complementary to our initial monitoring of M-phase cells (Figure 2) because our initial monitoring allowed us to detect the earliest germ cells to enter M-phase upon re-feeding, whereas this analysis allowed us to detect the slowest such cells. To detect M-phase entry of all cells, we blocked M-phase exit using a temperature sensitive mutation in *emb-30*, which encodes a component of the anaphase-promoting complex (Furuta et al., 2000). *emb-30(tn377ts)* hermaphrodites were starved at the permissive temperature (15˚), then shifted to the restrictive temperature (25˚) and re-fed. At the time of re-feeding, germlines contained a mixture

of S-phase and G2 cells (data not shown). In response to re-feeding, germ cells entered M phase, as expected, but were unable to complete the metaphase-to-anaphase transition, thus enabling us to quantify the accumulation of M-phase cells: Two hours after re-feeding, 55% of cells, on average, had entered M phase (n = 60 gonadal arms); after four hours, this number reached 99% (n = 66 gonadal arms) (Figure 6B). (This analysis is restricted to the distal-most 50 germ cells, because germ cells located more proximally sometimes directly entered the meiotic cell cycle upon re-feeding. See Figure 6.) Therefore, virtually all mitotically dividing germ cells completed the remainder of S phase and G2 within four hours of re-feeding, a time shorter than the time required to complete all of S phase and G2 in continuously fed adult hermaphrodites (~4.4-6.8 hours for S-phase, plus ~1.3-2.3 hours for G2). Thus, not only does re-feeding trigger germ cells arrested in G2 to enter M phase, but re-feeding also restores the rate of progression through S phase and earlier stages of G2.

Starvation-induced quiescence does not require proximity to the germline stem cell niche

Mitotically dividing germ cells in adults are confined to the distal gonad, where they contact a single somatic cell—the distal tip cell (or pair of distal tip cells, in males) (Figure 1A). The distal tip cell forms the niche for germline stem cells (Kimble and Seidel, 2013) and influences how germ cells respond to physiological cues (Dalfo et al., 2012). We therefore tested the effect of proximity to the distal tip cell on cell-cycle responses to food removal and re-feeding. We monitored M-phase cells, as above, in two mutant backgrounds in which mitotically dividing germ cells fill the gonad (i.e. germline tumors): (i) *glp-1(oz112gf)/Notch* gain-of-function mutants, in which constitutive GLP-1/Notch signaling maintains all germ cells in the mitotic cell cycle (Berry et al., 1997); and (ii) *gld-3(q730) nos-3(q650)* loss-of-function mutants, in which meiotic entry is inhibited irrespective of GLP-1/Notch signaling (Byrd et al., 2014; Eckmann et al., 2004). Germ cells in both genotypes of germline tumors responded normally to starvation and re-feeding: Outside the region normally corresponding to the progenitor zone (i.e. outside the distal-most 20 rows of germ cells), M-phase cells disappeared quickly in response to food removal and re-bounded one to two hours after re-feeding (Figure 4). These results demonstrate that proximity to the distal tip cell—the germline stem cell niche—is not required for a normal starvation and re-feeding response. Additionally, these results refine our understanding of the control of germ cell fate: Constitutive GLP-1/Notch signaling or combined loss of *gld-3* and *nos-3* does not promote germ cell proliferation *per se*, but rather promotes an

undifferentiated fate in which cells divide only in the presence of food.

Starvation-induced quiescence maintains germline stem cells independent of GLP-1/Notch

In multiple types of stem and progenitor cells, cell-cycle quiescence correlates with the capacity for long-term self-renewal (Cheung and Rando, 2013; Orford and Scadden, 2008). We therefore investigated how quiescence affects the maintenance of *C. elegans* germline stem cells. Under fed conditions, maintenance of these stem cells requires GLP-1/Notch signaling (Austin and Kimble, 1987). The *glp-1* gene, which encodes one of two Notch receptors in *C. elegans*, is expressed in the progenitor zone, and the receptor is activated by ligands expressed in the adjacent distal tip cell (Henderson et al., 1994; Kimble and Crittenden, 2007; Nadarajan et al., 2009). We used the temperature-sensitive *glp-1* allele *q224ts* to test whether GLP-1/Notch signaling is similarly required for maintenance of germline stem cells under starved conditions. The *q224ts* allele is the strongest of all known temperature-sensitive *glp-1* alleles and behaves like a null at the restrictive temperature (Austin and Kimble, 1987; Kodoyianni et al., 1992).

In fed animals, removal of GLP-1/Notch signaling causes germline stem cells to be lost: Stem cells fail to self-renew, and instead all germ cells enter the meiotic cell cycle (Austin and Kimble, 1987; Cinquin et al., 2010; Fox and Schedl, 2015). We tested whether loss of GLP-1/Notch signaling produces these same effects in starved animals. We removed food from *glp-1(q224ts)* hermaphrodites at the permissive temperature (15˚), shifted starved animals to the restrictive temperature (25˚) for eight hours, then evaluated germ cell fate. Cell fate was assessed by staining for the meiosis-associated protein GLD-1 (Jones et al., 1996) and by scoring cells for the 'crescent' chromosome morphology indicative of meiotic chromosome pairing (Dernburg et al., 1998). This morphology is readily distinguishable from the 'non-crescent' morphology found in mitotic interphase. In fed controls, incubation at the restrictive temperature caused all germ cells to enter the meiotic cell cycle: Chromosomes adopted the 'crescent' shape (Figure 5A), and GLD-1 levels in the distal-most germ cells rose (Figure 5I). In starved animals, by contrast, meiotic entry did not occur: 99% (n = 214) of progenitor zones retained germ cells with an interphase chromosome morphology (Figure 5C), and GLD-1 levels in the distal-most germ cells remained low (n = 47 of 47 gonadal arms) (Figure 5I). Importantly, germ cells in starved animals retained the capacity for mitotic cell division, because when starved animals were re-fed at the restrictive temperature, their germ cells re-entered M phase (Figure 5G). Germ cells in starved animals also retained the capacity for long-term self-renewal, because when starved animals

were instead returned to the permissive temperature and re-fed for two to three days, 91% (n = 148) of progenitor zones retained germ cells in the mitotic cell cycle (Figure 5C). Similar results were observed when incubation at the restrictive temperature was extended to 16 or 24 hours (Figure 5D). These results demonstrate that starved animals maintain germline stem cells independent of GLP-1/Notch. In other words, starvation inhibits the meiotic entry of germline stem cells, even in absence of GLP-1/Notch. Like cell-cycle quiescence, this inhibition of meiotic entry was reversible upon re-feeding, because when starved *glp-1(q224ts)* animals were re-fed at the restrictive temperature, all germ cells eventually entered the meiotic cell cycle (Figure 5H).

Quiescence induced by non-starvation conditions maintains germline stem cells independent of GLP-1/Notch

To further investigate the relationship between cell-cycle quiescence and stem cell maintenance, we asked, apart from starvation, do other conditions that inhibit germ cell division also maintain germline stem cells independent of GLP-1/Notch? To answer this question, we performed temperature-shift experiments in *glp-1(q224ts)* hermaphrodites under two additional conditions: High NaCl and absence of sperm, each of which causes a two-fold drop in the germ cell mitotic index (Morgan et al., 2010; Salinas et al., 2006). Animals exposed to high NaCl (300 mM) or lacking sperm (via loss-of-function mutation in *fog-1*) were grown at the permissive temperature, shifted to the restrictive temperature for eight hours, then returned to the permissive temperature for two to three days. Following this treatment, germ cell fate (mitotic versus meiotic) was evaluated by scoring germ cells for the 'crescent' chromosome morphology indicative of meiotic prophase (described above). For both high NaCl and absence of sperm, 48-79% (n = 129-231) of gonadal arms retained germ cells in the mitotic cell cycle (Figure 5E-F). As a control for possible pleiotropic effects of the mutation used to eliminate sperm (*q785*), sperm was introduced to *fog-1(q785); glp-1(q224ts)* animals by mating with wildtype males, and these animals were examined in parallel. In such animals, incubation at the restrictive temperature caused all germ cells to enter the meiotic cell cycle (data not shown; n = 37 gonadal arms, scored immediately following incubation at the restrictive temperature). Thus, three stress conditions that inhibit or reduce germ cell division (starvation, high NaCl, absence of sperm) also permitted maintenance of germline stem cells independent of GLP-1/Notch. This commonality suggests that cell-cycle quiescence itself is an effector of stem cell maintenance

(Figure 5J). Nonetheless, such maintenance is not simply a function of inhibiting passage through M-phase, because stem cell maintenance in absence of GLP-1/Notch was not permitted by cell-cycle arrest caused by RNAi knockdown of cyclin-dependent kinase 1 (*cdk-1*) (Figure 5B), a result we confirmed by visualizing formation of the synaptonemal complex (Figure5—figure supplement 1).

Starvation inhibits the meiotic entry of transient progenitors

The results above demonstrate that starvation inhibits the meiotic entry of germline stem cells, even in absence of GLP-1/Notch. We therefore hypothesized that starvation might also control the meiotic entry of transient progenitors, located in the proximal progenitor zone (Figure 1A). No markers currently exist to distinguish transient progenitors from germline stem cells, and the boundary between these pools of cells is not clear, but the two pools can be distinguished under fed conditions by restricting movement of cells out of the progenitor zone(Cinquin et al., 2010). Under such conditions, transient progenitors enter the meiotic cell-cycle, whereas germline stem cells do not (Cinquin et al., 2010). To compare meiotic entry of transient progenitors under fed versus starved conditions, we re-fed starved animals and restricted cell movement during re-feeding; we then compared meiotic entry after re-feeding to meiotic entry after continued starvation. Meiotic entry was assessed by staining for GLD-1 and by scoring cells for the 'crescent' chromosome morphology indicative of meiotic prophase (described above). Cell movement was restricted by performing this experiment in *emb-30(tn377ts)* hermaphrodites at the restrictive temperature (25˚), a condition that induces metaphase arrest (also described above, under 'Re-feeding restores the rate of…') (Furuta et al., 2000). *emb-30(tn377ts)* animals were starved at the permissive temperature (15˚), shifted to the restrictive temperature (25˚), then re-fed for six hours or maintained in starvation. Our primary result from this experiment was that re-feeding and continued starvation affected meiotic entry differently. After six hours of re-feeding, cells in the proximal (but not distal) progenitor zone entered the meiotic cell cycle: GLD-1 levels in the proximal half of the progenitor zone rose (Figure 6A), and the boundary between 'crescent' and 'non-crescent' germ cells moved distally, such that the number of cells distal to this boundary was reduced by about half (Figure 6C). After six hours of continued starvation, by contrast, very little meiotic entry was observed: GLD-1 levels in the proximal progenitor zone remained largely unchanged (Figure 6A), and the number of cells distal to the 'crescent'/'non-crescent' boundary was only slightly reduced (Figure 6C). Our

inference from these results is that the proximal half of the progenitor zone was composed of transient progenitors at the start of re-feeding, and that six hours of re-feeding—but not six hours of continued starvation—allowed for their timely progression into the meiotic cell cycle. We conclude that starvation slows or blocks the meiotic entry of transient progenitors, similar to its effect on the meiotic entry of germline stem cells.

Starvation-induced quiescence is distinct from cell-cycle arrest induced by DNA-damage

As a first step towards understanding the regulation of cell-cycle quiescence induced by starvation, we compared this quiescence to cell-cycle arrest caused by DNA damage, another perturbation causing G2 arrest (Gartner et al., 2000; Kuntz and O'Connell, 2009). By three criteria, starvation-induced quiescence was distinct from cell-cycle arrest caused by DNA damage. First, DNA damage strongly up-regulates inhibitory phosphorylation of CDK-1 (Figure 7A; Craig et al., 2012). By contrast, starvation-induced quiescence did not up-regulate this phosphorylation (Figure 7A). Second, DNA damage causes germ cell nuclei to enlarge (Figure 7A; Gartner et al., 2000), a phenotype replicated by RNAi knockdown of *cdk-1* (Jeong et al., 2011). By contrast, starvation-induced quiescence did not cause nuclei to enlarge (Figure 7A). Third, cell-cycle arrest in response to DNA damage requires the p53 homolog *cep-1* (Derry et al., 2007). By contrast, starvation-induced quiescence did not require *cep-1* (Figure 7B). We conclude that starvation and DNA damage induce cell-cycle arrest differently.

Starvation-induced quiescence does not require factors affecting larval and behavioral responses to food

As a second step towards understanding the regulation of starvation-induced quiescence, we tested whether this quiescence requires factors influencing the larval germline's response to food (Dalfo et al., 2012; Michaelson et al., 2010), including factors controlling germ cell quiescence during the two larval diapause states—L1 diapause (Fukuyama et al., 2006; Fukuyama et al., 2012) and the mid-larval Dauer diapause (Narbonne and Roy, 2006). Food was removed from early adult hermaphrodites homozygous for mutations in the TGF-β pathway, the insulin/insulin-like growth factor 1 (IGF-1) pathway, or the AMPK pathway. M-phase cells were then monitored after food removal. Additionally, to test for a requirement for factors affecting behavioral responses to food, this same experiment was performed in animals defective for neuropeptide processing, neuropeptide secretion, or chemosensation, as well as in animals exposed to exogenous serotonin, which in some contexts acts as a food signal (Luedtke et al.,

2010). In all experiments, M-phase cells disappeared quickly in response to food removal (Figure 7B). We conclude that each of the genes tested is not individually required for starvation-induced quiescence in adult germ cells, and that quiescence is not affected by exogenous serotonin. These findings suggest that quiescence in adults is controlled differently than cell-cycle responses in the larval germline and is largely independent of behavioral responses to food. These results are consistent with adult versus larval germ cells responding to food removal differently (Figure 2A versus C) and with reduced insulin/IGF-1 signaling or TGF-β signaling not affecting the germ cell mitotic index in fed adult hermaphrodites (Dalfo et al., 2012; Michaelson et al., 2010). Likewise, these results are consistent with no requirement for *daf-16/FOXO* in reducing the proliferation of *Drosophila* germline stem cells in response to poor diet (Hsu et al., 2008).

Discussion

This work establishes the adult germline of *C. elegans* as model for studying the facultative quiescence of stem cells *in vivo* and demonstrates that cell-cycle quiescence can maintain the stem cell fate, independent of a key signaling pathway otherwise required for this fate. Briefly, we find that in the absence of food, adult germ cells in *C. elegans* stop dividing and become quiescent. This quiescence is characterized by a slowing of S phase and a block to M-phase entry, such that cells arrest in the G2 phase of the cell cycle. Further, this quiescence maintains germline stem cells independent of GLP-1/Notch, a signal required for stem cell maintenance under conditions of active proliferation. Re-feeding causes germ cells to exit quiescence rapidly, and a requirement for GLP-1/Notch signaling similarly resumes.

Cell-cycle quiescence promotes stem cell maintenance

Cell-cycle quiescence was once thought to be a near universal feature of stem cells in adult tissues (Hall and Watt, 1989; Potten and Loeffler, 1990). This view arose from the theory that biological systems ought to protect stem cells from the risks of DNA replication and led to the notion of quiescence as an inherent property of the stem cell fate. According to this model, tissues were maintained by a hierarchy of relatively quiescent master stem cells and their faster-cycling but short-lived daughters. In recent years, however, work in several mammalian and invertebrate tissues has shown that quiescence is not a prerequisite for the stem cell fate (Barker et al., 2010a; Crittenden et al., 2006; Doupe and Jones, 2013; Fuchs, 2009; Maciejowski et al., 2006; Simons and Clevers, 2011). Some types of stem cells do not exhibit quiescence under

conditions assayed (e.g. Barker et al., 2010b; de Navascues et al., 2012; Snippert et al., 2010), and still others vary their cell-cycle length in accordance with the physiological circumstances surrounding them (e.g. Harrison and Lerner, 1991; Hartman et al., 2013; Lugert et al., 2010; Qiao et al., 2007). Nevertheless, genetic or environmental perturbations that impact the cell cycle can also affect stemness (Orford and Scadden, 2008; Pietras et al., 2011; Yilmaz et al., 2012). Thus, a long-standing question in the field of stem cell biology has remained: Does cell-cycle quiescence play a role in maintaining the stem cell fate? Our results answer this question by showing that quiescence itself alters the genetic requirements for stemness: Actively dividing germline stem cells in *C. elegans* require GLP-1/Notch signaling for their maintenance (Austin and Kimble, 1987); we find that cell-cycle quiescence—induced by starvation, high NaCl, or absence of sperm—relieves this requirement (Figure 5J). Thus, cell-cycle quiescence maintains germline stem cells independent of the signal required for such maintenance under conditions of active proliferation.

The molecular mechanisms maintaining stem cells during periods of cell-cycle quiescence remain to be determined. Acting downstream of GLP-1/Notch signaling to maintain germline stem cells are the PUF-family translational repressors FBF-1 and FBF-2 (Crittenden et al., 2002) and the proteins of unknown molecular function LST-1 and SYGL-1 (Kershner et al., 2014). Quiescence might stabilize these stem cell regulators—for example, by inhibiting the protein degradation machinery linked to the cell-cycle. Alternatively, quiescence might substitute for the repressive effects of FBF-1 and FBF-2 by repressing translation on a global level. Global repression of translation is a conserved stress response (Spriggs et al., 2010), and the stress of starvation represses translation of at least a few genes in *C. elegans* (Lascarez-Lagunas et al., 2014). Another possibility is that stem cell maintenance might be regulated by a metabolite or metabolic process whose levels change during quiescence. Such connections between metabolism and developmental processes have been observed in a variety of vertebrate and invertebrate cell types (Agathocleous and Harris, 2013).

Control of the G2-to-M transition by nutrients or growth factors may be a broadly conserved feature of the eukaryotic cell cycle

We find that adult germ cells in *C. elegans* do not arrest in G1 during starvation but instead progress slowly through S phase and arrest in G2. Most eukaryotic cells can transiently pause in G2 in response to DNA damage or microtubule disassembly (Rieder, 2011), but the G2-

to-M transition has not been viewed as a point of cell-cycle control in response to growth factors or nutrients, largely because early studies in mammalian tissue culture showed that cell-cycle events in fibroblasts become independent of extracellular cues after entry into S phase (Pardee, 1989). Despite this view, the G2-to-M transition is emerging as the primary point of cell-cycle control in *C. elegans* germ cells, and the G2-to-M transition also responds to growth factors or nutrients in other systems.

C. elegans germ cells arrest in G2 in embryonic development (Fukuyama et al., 2006) and two larval diapause states—L1 diapause (Fukuyama et al., 2006) and Dauer (Narbonne and Roy, 2006). Our results show that G2 arrest also occurs in starved adults (Figure 3C), and that the length of G2 can vary more than 8-fold even under well-fed conditions (Figure 3—figure supplement 1). At the same time, G1 is very short (Fox et al., 2011, Figure 3—figure supplement 1), and cyclin E/cyclin-dependent kinase 2, which drives the G1-to-S transition (Orford and Scadden, 2008), is active throughout the cell cycle (Fox et al., 2011). These observations support a model of cell-cycle control in *C. elegans* germ cells in which regulation in response to extracellular cues relies on the G2-to-M transition.

G2 arrest in response to nutrient limitation has also been observed for fission yeast (Costello et al., 1986), budding yeast (Laporte et al., 2011), and *Tetrahymena* (Cameron and Bols, 1975). Moreover, the G2-to-M transition is a point of cell-cycle control in response to poor nutrient conditions in germline stem cells of *Drosophila* (Hsu et al., 2008; LaFever et al., 2010; Roth et al., 2012). Even under replete conditions, germline stem cells in *Drosophila* are thought to be paused in G2 (Morris and Spradling, 2011), as are a substantial fraction of *Drosophila* intestinal stem cells (Zielke et al., 2016). In mammals, cells can pause in G2 for prolonged periods of time before dividing in response to various stimuli (e.g. wounding, hormones) (reviewed in Gelfant, 1977). Such pausing in mammals has not been the subject of recent investigation, although the G2-to-M transition is known to be regulated by the growth factor IGF-1—for example, in mammalian uterine cells (Adesanya et al., 1999), oligodendrocyte progenitors (Frederick and Wood, 2004; Min et al., 2012), spermatogonial stem cells (Wang et al., 2015), and multiple myeloma cells (Stromberg et al., 2006). Proper timing of the G2-to-M transition is also essential during development (reviewed in Bouldin and Kimelman, 2014), with some populations of cells naturally held in G2 in both *Drosophila* and zebrafish (e.g. Bouldin et

al., 2014; Usai and Kimura, 1992). Thus, control of the G2-to-M transition by growth factors or nutrients may be a conserved feature of the eukaryotic cell cycle.

C. elegans germline is a model for tissue plasticity and facultative stem cell quiescence

Tissues in adult organisms can be remarkably plastic in their ability to shrink and re-grow in response to changing physiological demands (e.g. Bergtold, 1926; Secor and Diamond, 1998). Such plasticity requires broad flexibility in a range of cellular behaviors, yet our understanding of tissue plasticity on a cellular level is limited, primarily because tractable models of tissue plasticity are only now being developed (e.g. O'Brien et al., 2011). The *C. elegans* germline presents such a model. This tissue undergoes dramatic shrinkage in adult hermaphrodites starved from the L4 larval stage, and such shrinkage is reversible upon re-feeding (Angelo and Van Gilst, 2009; Seidel and Kimble, 2011). Previous studies showed that germline shrinkage occurs in part through programmed cell death and oogenesis (Angelo and Van Gilst, 2009; Seidel and Kimble, 2011). This work establishes facultative stem cell quiescence as a third major force: Because germ cells stop dividing during starvation, cells lost to cell death and oogenesis are not replaced, thus causing the germline tissue to shrink. Quiescence also contributes to re-growth during re-feeding by ensuring that germ cells are able to re-enter the cell cycle rapidly in response to food. Rapid exit from quiescence is a characteristic shared by analogous re-feeding responses in other animals, at least in the handful of examples where such responses have been examined at short timescales—for example, in the ovary of protein-limited *Drosophila* (Hartman et al., 2013; Jouandin et al., 2014), in the gut of fasted rats, squirrels, and chicks (Aldewachi et al., 1975; Cameron and Cleffmann, 1964; Hagemann and Stragand, 1977; Kruman et al., 1988), and in the retina of yolk-deprived frog embryos (Love et al., 2014). These observations stand in contrast to the comparatively longer times required for exit from quiescence in mammalian tissue culture (Lum et al., 2005; Pardee, 1974; Soprano, 1994; Zetterberg and Larsson, 1985) and suggest that *in vivo* models of quiescence may uncover new mechanisms of cell-cycle control.

Materials and methods

Strains

N2, CB4856 (Hodgkin and Doniach, 1997), TJ1 *cep-1(gk138) I* (Consortium, 2012), TG38 *aak-2(gt33) X* (Lee et al., 2008), RB754 *aak-2(ok524) X* (Narbonne and Roy, 2006), JK5399 *aak-1(tm1944) III; aak-2(ok524) X* (Fukuyama et al., 2012), MR507 *aak-2(rr48) X* (Narbonne and Roy, 2006), JK326 *par-4(it57ts) V* (Watts et al., 2000), GR1310 *akt-1(mg144gf) V* (Paradis and Ruvkun, 1998), CF1038 *daf-16(mu86) I* (Lin et al., 1997), NS3227 *daf-18(nr2037) IV* (Mihaylova et al., 1999), RB712 *daf-18(ok480) IV* (Fukuyama et al., 2006) , JK5011 *daf-3(e1376) X* (Patterson et al., 1997), JK4971 *daf-5(e1386) II* (da Graca et al., 2004), IK130 *pkc-1(nj3) V* (Sieburth et al., 2007), CB169 *unc-31(e169) IV* (Speese et al., 2007), KP2018 *egl-21(n476) IV* (Husson et al., 2007), MT1241 *egl-21(n611) IV* (Husson et al., 2007), VC461 *egl-3(gk238) V* (Husson et al., 2006), VC671 *egl-3(ok979) V* (Husson et al., 2006), JK4963 *bbs-5(gk507) III* (Lee et al., 2011), JK4962 *bbs-5(gk537) III* (Lee et al., 2011), JK4960 *bbs-8(nx77) V* (Blacque et al., 2004), JK4964 *bbs-9(gk471) III* (Chen et al., 2006), JK4970 *tom-1(ok285) I* (Gracheva et al., 2006), CB1377 *daf-6(e1377) X* (Perens and Shaham, 2005), BS860 *unc-32(e189) glp-1(oz112gf) / dpy-19(e1259) glp-1(q172) III* (Berry et al., 1997), JK3182 *gld-3(q730) nos-3(q650) / mIn1[mIs14 dpy-10(e128)] II* (Eckmann et al., 2004), JK5098 *fog-1(q785) I / hT2[qIs48](I;III); glp-1(q224ts) III / hT2[qIs48](I;III)* (Morgan et al., 2010), JK5336 *weSi2[Pmex-5::gfp::his-58::tbb-2 3' UTR; Cbr-unc-119(+)] II; emb-30(tn377ts) III* (Furuta et al., 2000), JK4605 *glp-1(q224ts) III* (Kodoyianni et al., 1992)

Worm maintenance, synchronization, and staging

Unless otherwise noted, worms were maintained on nematode growth media spotted with *E. coli* OP50 at 20˚C. Nematode growth media contained 3 g/L NaCl, 2.5 g/L peptone, 20 g/L agar, 25 ml/L 1 M Potassium Phosphate Buffer (1 M K_2HPO_4 mixed with 1 M KH_2PO_4 to reach a pH of 6.0), 1 mM $CaCl_2$, 1 mM $MgSO_4$, 5 µg/ml cholesterol, and 2 µg/ml uracil. Worms were synchronized by bleaching gravid hermaphrodites for 5-8 minutes in a 1 : 2 : 12 solution of 5 M NaOH : household bleach : M9 (3 g/L KH_2PO_4, 6 g/L $NaHPO_4$, 5 g/L NaCl, 1 mM $MgS0_4$). Embryos were allowed to hatch overnight in M9 in an aerated flask, with shaking at ~170 rpm. L1 larvae were then plated onto 10 cm plates, at a density of ~1,000 per plate, and grown to the appropriate developmental stage.

We staged animals as 'early adult' when hermaphrodites had molted into adulthood and recently begun to ovulate, with most hermaphrodites containing 1 or 2 embryos in utero, but with some hermaphrodites containing zero embryos or up to 4 embryos. Animals with germline tumors (and therefore no ovulation) were staged according to the ovulation-status of their non-tumorous siblings. At 20˚C, early adulthood was reached ~48-52 hours after L1 feeding. For staging of L4 animals, we examined the extent to which the hermaphrodite gonad had migrated from the loop towards the vulva. We define populations as 'early L4' when the gonad had migrated ~1/4 of this distance and 'mid-L4' when the gonad had migrated ~1/2-3/4 of this distance. Males were staged according their hermaphrodite siblings.

Food removal and re-feeding

Food was removed by gently washing animals from bacterially seeded plates with M9, pelleting animals by spinning at 100-200 g for ~1 min, then washing animals 3-6 additional times with M9, using 15 ml M9 per wash per 1,000-3,000 animals. Animals were then deposited onto unseeded 10 cm plates and gently spread across plates such that all liquid was absorbed into the plate within 5 minutes. Media for starvation plates contained 3 g/L NaCl, 25 g/L agar, 25 ml/L 1 M Potassium Phosphate Buffer (see above), 1 mM $CaCl_2$, 1 mM $MgSO_4$, and 5 µg/ml cholesterol. This starvation procedure lasted ~10-15 minutes from start to finish, with time zero being the moment at which M9 was first added to the bacterially seeded plates. Mock food removal was performed the same, except that animals were washed in M9 + ~0.5% OP50 and deposited onto bacterially seeded plates. In most experiments, animals were starved at densities of 500-1,000 animals per 10 cm plate. Exceptions were starvations beginning from L4, in which animals were starved at densities of 2,000-3,000 per 10 cm plate, and experiments requiring that animals be hand-picked, in which animals were starved at densities of less than 500 per 10 cm plate.

Re-feeding was performed by washing animals from starvation plates with M9 + ~0.5% OP50, spinning at 100-200 g for ~1 min to pellet animals, then depositing animals onto 10 cm nematode growth media plates seeded with OP50. Animals were spread across the plate such that all liquid was absorbed into the plate within 5 minutes.

Genotypes requiring non-standard growth conditions

glp-1(q224ts) and *fog-1(q785); glp-1(q224ts)*: Animals were grown at 15˚C. All plates and M9 solutions used to handle animals were pre-equilibrated to 15˚C. Animals were

synchronized as described above, but the bleaching protocol was modified, as follows, because *glp-1(q224)* embryos are bleach-sensitive. Gravid hermaphrodites were incubated in bleaching solution for ~1 minute, to kill the adult hermaphrodites but allow their carcasses to remain intact. Embryo-containing carcasses were incubated at 15˚C for 4-8 hours. Carcasses were then bleached again, for 3-4 minutes, to liberate embryos. Hatching of L1s in M9 and was performed at 15˚C and extended to 36-40 hours, to account for longer embryonic development times at 15˚C. At 15˚C, animals reached the early adult stage ~90-96 hours after L1 feeding.

par-4(it57ts): Animals were grown at 15˚C until the L3 stage, then shifted to 25˚C until animals reached early adult. The *par-4(it57ts)* starvation timecourse was performed at 25˚C.

aak-1(tm1944); aak-2(ok524): Animals were grown at 15˚C until the early L4 stage, then transferred to 20˚C until animals reached early adult. Growth at 15˚C was used because *aak-1(tm1944); aak-2(ok524)* animals grown at 20˚C showed high sterility. Additionally, an alternate synchronization protocol was used because hatching of *aak-1(tm1944); aak-2(ok524)* L1s in M9 causes sterility (Fukuyama et al., 2012). Early adults were bleached according to the protocol described for *glp-1(q224ts)*, and embryos were deposited directly onto food.

emb-30(tn377ts): Animals were grown at 15˚C prior to temperature shifts.

Antibody and DAPI staining

Gonads were dissected in M9 + 0.1% Tween-20 + 0.25 mM levamisole. For GLD-1 and phospho-histone H3 staining, gonads were fixed in PBS + 3% paraformaldehyde + 0.1% Tween-20 (PBSTween) for 30 minutes, followed by -20˚C methanol for 15 minutes (anti-GLD-1 and anti-HIM-3) or ≥ 15 minutes (anti-phospho-histone H3). For phospho-CDK-1 staining, gonads were fixed in PBSTween + 3.7% formaldehyde for 10 min, followed by -20˚C methanol for 5 min. Gonads were blocked for 30 minutes at room temperature in PBSTween + 3-5% normal donkey serum (anti-GLD-1 and anti-phospho-CDK-1) or 1-3% bovine serum albumin (anti-HIM-3 and phospho-histone H3). Incubations with primary antibodies were performed overnight at 4˚C, with antibodies diluted in blocking solution. Dilutions were as follows: mouse anti-phosopho-histone H3 (Cell Signaling #9706), 1/150; rabbit anti-GLD-1 (Cinquin et al., 2010), 1/100; rabbit anti-HIM-3 (Novus Biologicals #53470002), 1/200; rabbit anti-phospho-CDK-1 Thr14/Tyr15 (Santa Cruz #sc-28435-R) (Rahman et al., 2014), 1/200; rabbit anti-phospho-CDK-1 Tyr15 (Calbiochem #219440) (Hachet et al., 2007), 1/100. Incubations with secondary antibodies were performed for 1-2 hours at room temperature, using Cy-3 donkey anti-mouse

(Jackson ImmunoResearch #715-165-151) or Cy-3 donkey anti-rabbit (Jackson ImmunoResearch # 711-165-152), diluted 1/1,000. Gonads were mounted in Vectashield containing DAPI (Vector Labs #H-1200). For DAPI staining in absence of antibody staining, gonads were fixed as for phospho-histone H3 staining, then mounted in Vectashield containing DAPI.

To test the phospho-specificity of anti-phospho-CDK-1, gonads were dissected and fixed, as above, and after fixation, gonads were treated with 20 U/µl Lambda Protein Phosphatase (NEB #P0753S) in Protein MetalloPhosphatase Buffer (50 mM HEPES pH 7.5, 100 mM NaCl, 2 mM DTT, 0.01% Brij 35, 1 mM $MnCl_2$) for 1 hour at 30˚C. Control gonads were treated the same, but Lambda Protein Phosphatase was omitted from the reaction. Gonads were then blocked and stained with anti-phospho-CDK-1, as above.

Imaging

Unless otherwise noted, images were obtained on a Leica SP8. In all experiments, identical imaging conditions and brightness adjustments were used across samples.

Counting M-phase cells

Unless otherwise noted, M-phase cells were scored by examining gonads for phospho-histone $H3^+$ cells at 63X magnification. In all experiments, a subset of gonads was examined via DAPI staining, to confirm the correspondence between phospho-histone $H3^+$ cells and mitotic figures. In germline tumors, M-phase cells occurring in the distal-most 20 rows of germ cells (i.e. the region corresponding to the progenitor zone in wildtype gonads) were excluded from analysis. Additionally, we excluded germline tumors with patches of differentiation (as assessed by DAPI staining), which sometimes occurred in *glp-1(oz112gf)* animals.

EdU labeling

EdU labeling was performed by soaking or by feeding. Soaking was used for starvation timecourses (Figure 3A) and for testing whether G1 versus G2 cells could be distinguished by nuclear size (Figure 3—figure supplement 2). Feeding was used for measurements cell-cycle length in fed animals (Figure 3—figure supplement 1). For the soaking procedure, animals were incubated with rocking in M9 + 0.1% Tween-20 + 1 mM EdU for 15 minutes at room temperature. Gonads were dissected as for antibody staining and fixed in 3% paraformaldehyde in PBSTween for 30 minutes, followed by -20˚C methanol for ≥ 15 minutes. Gonads were blocked in PBSTween + 3% bovine serum albumin for 30 minutes at room temperature. Click-iT

reactions were performed using the Click-iT EdU Alexa Fluor 488 Imaging Kit (Invitrogen #C10337), according to the manufacturer's instructions, except that two back-to-back half reactions of 250 µl volume were performed. Gonads were mounted in Vectashield containing DAPI.

EdU labeling by feeding was performed similar to previous studies (Crittenden et al., 2006; Fox et al., 2011; Morgan et al., 2010). *E. coli* strain MG1693 was grown overnight at 37˚C in M9 minimal media (3 g/L KH_2PO_4, 6 g/L Na_2HPO_4, 0.5 g/L NaCl, 1 g/L NH_4Cl, 2 mM $MgSO_4$, 0.1 mM $CaCl_2$, 0.4% glucose, 1 µg/ml thiamin) supplemented with 5 µg/ml thymine. This culture was diluted 1:50 in M9 minimal media supplemented with 0.5 µM thymidine and 20 µM EdU and grown for 32 hours at 37˚C. Cells were re-suspended in ~1/100th of their original volume in M9, then spread onto 6 cm plates, using 100 µl of *E. coli* solution per plate. Plate media was identical to standard nematode growth media except that 60 µg/ml carbenicillin was added, peptone was omitted, and agar was exchanged for 12 g/L agar + 6 g/L agarose. Plates were seeded one day prior to adding worms. Worms were transferred to plates for the required period of time, then gonads were dissected and processed as above.

Propidium iodide staining and its quantification

EdU-labeled gonads were stained with propidium iodide to measure DNA content and to allow for simultaneous imaging of Alexa Fluor 488 and DNA. Propidium iodide staining was performed by adding two steps to the aforementioned EdU-labeling protocol. First, prior to the blocking step, gonads were incubated in PBSTween + 20 µg/ml RNase A for 1 hour at 37˚C. Second, after the Click-iT reaction, gonads were incubated for 30 minutes at room temperature in PBSTween + 50 µg/ml propidium iodide.

To quantify propidium iodide staining, gonads were imaged at 63X magnification on a Zeiss LSM510 laser-scanning confocal microscope, with a z-stack interval of 0.37-0.39 µm. Pixel intensity per nucleus was calculated as the summation of all pixel intensities within a best-fit cylinder whose height matched the height of the focal nucleus in the z-dimension and whose cross-sectional diameter matched the largest dimension of the focal nucleus in the x-y dimension. Cylinders were defined manually by drawing circles around nuclei in ImageJ. This quantification method is undeniably crude because cylinders often included portions of neighboring nuclei. Nevertheless, this method allowed us to distinguish non-S-phase cells as having a DNA content

632 less than S-phase cells (G1) or a DNA content greater than S-phase cells (G2) (Figure 3—figure
633 supplement 2).
634 **Use of nuclear size to distinguish G1 versus G2 cells**
635 Cells were classified as G1, S-phase, or G2 by a combination of EdU labeling (to mark S-
636 phase cells) and nuclear size. This method has not been used previously—although others have
637 noted a correlation between cell-cycle stage and nuclei size (Chiang et al., 2015; Fukuyama et
638 al., 2006; Lawrence et al., 2015)—and we justify its use here. In pilot experiments involving
639 EdU labeling and DNA quantification, we noticed a correlation between cell-cycle stage and
640 nuclear size: G1 and early S-phase nuclei were small, G2 and late S-phase nuclei were large, and
641 mid S-phase nuclei were intermediate in size (Figure 3—figure supplement 2). Additionally, G1
642 nuclei nearly always occurred in pairs, consistent with G1 being very short (Fox et al., 2011).
643 The size difference between G1 and G2 nuclei was large enough that in EdU-labeled gonads, G1
644 and G2 nuclei could be distinguished by eye ($n > 100$ nuclei, from a total of seven progenitor
645 zones). To test the accuracy of this method more thoroughly, we obtained z-stack images of
646 EdU-labeled, propidium iodide-stained progenitor zones from three fed early adult
647 hermaphrodites and three hermaphrodites starved from early adult for 3.5 hours. We first
648 classified each cell as S-phase (EdU^+), G1 (EdU^- and having a nuclear size equal to or smaller
649 than the smallest EdU^+ cells), or G2 (EdU^- and having a nuclear size equal to or larger than the
650 largest EdU^+ cells). We then quantified propidium iodide staining (a measure of DNA content)
651 and compared our 'by size' classification to the classification given by propidium iodide staining
652 (Figure 3—figure supplement 2). For all cells in all six progenitor zones, the two classification
653 systems matched perfectly (Figure 3—figure supplement 2). We therefore used the 'by size'
654 classification system for counting G1, S-phase, and G2 cells throughout.
655 **Counting G1, S-phase, and G2 cells**
656 EdU-labeled progenitor zones were imaged at 63X magnification with a z-stack interval
657 of 1 μm. Cells were counted as belonging to the progenitor zone if they had an interphase or M-
658 phase chromosome morphology and if their midpoint was located distal to a cross-sectional line
659 drawn through the midpoint of the second most distal 'crescent' cell (i.e. the second most distal
660 meiotic prophase cell). Progenitor-zone cells were classified as G1 (EdU^- and nuclear size equal
661 to or smaller than the smallest EdU^+ cells), S-phase (EdU^+), G2 (EdU^- and nuclear size equal to
662 or larger than the largest EdU^+ cells), or M-phase (mitotic figures). Classifications were recorded

using the Cell Counter plug-in for ImageJ (rsb.info.nih.gov/ij/plugins/cell-counter.html), by marking each cell in all z-slices in which it was observed. A custom R script was then used to identify marks belonging to the same cell.

Measuring cell-cycle parameters in fed animals

Cell-cycle parameters in fed animals were determined by first measuring the length of G2. G2 was measured by labeling animals with EdU (via feeding) and calculating the fraction of M-phase cells (mitotic figures) that were EdU^+ over time (equation 1, below). Next, the length of G2 was combined with the G2 index to calculate the total length of the cell cycle (equation 2). The lengths of G1, S-phase, and M-phase were calculated by multiplying the total length of the cell cycle by the G1, S-phase, or M-phase index (equations 3-5). Calculations of the maximum total length of the cell cycle depend on assumptions about covariance between the length of G2 and the length of M + G1 + S. If cells having a longer G2 are assumed to have a proportionally longer M + G1 + S, then the maximum length of the cell-cycle for 95% or 100% of cells is given by equation 6. If cells having a longer G2 are not assumed to have a proportionally longer M + G1 + S, then the maximum length of the cell-cycle for 95% or 100% of cells is given by equation 7. We performed both calculations.

(1) Median length of G2 = Time at which 50% of M-phase cells were EdU^+

(2) Median total length of cell cycle = Median length of G2 / G2 index

(3) Median length of G1 = Median total length of cell cycle * G1 index

(4) Median length of S-phase = Median total length of cell cycle * S-phase index

(5) Median length of M-phase = Median total length of cell cycle * M-phase index

(6) Maximum total length of cell cycle for 95% or 100% of cells = Time at which 95% or 100% of M-phase cells were EdU^+ / G2 index

(7) Maximum total length of cell cycle for 95% or 100% of cells = Median total length of cell-cycle * (M + G1 + S index) + time at which 95% or 100% of M-phase cells were EdU^+

Cell-cycle length in fed animals was measured in early adult hermaphrodites and in adult hermaphrodites aged 24 hours post mid-L4. For calculations involving early adults, indices for each cell-cycle phase were derived from the 0-hour timepoint of the timecourse in Figure 3. For calculations involving animals aged 24 hours post mid-L4, indices were derived from the 0.5-

hour timepoint of the timecourse in Figure 3—figure supplement 1, for consistency with (Fox et al., 2011).

Measuring distance from the gonad distal tip to the first 'crescent' germ cell

Gonads were stained with DAPI and examined at 63X magnification. In a central focal plane, one edge of the gonad was chosen at random, and the distal-most 'crescent' germ cell along that edge was identified. The number of germ cells (along the gonad edge) between this first 'crescent' cell and the distal tip of the gonad was counted.

UV treatment

L4 hermaphrodites close to the adult molt were transferred to an unseeded plate and exposed to 100 J/m^2 of 254 nm UV light in Spectrolinker XL-1000 UV Crosslinker. Animals were immediately returned to food and incubated for 8 hours at 20˚C before dissection. Animals were adults at the time of dissection.

Serotonin exposure

Serotonin creatinine sulfate was dissolved in M9 to a concentration of 50 mg/ml. This solution was spread onto starvation plates to a final concentration of 20 mM serotonin. Plates were incubated for at least one hour before worms were added. To expose animals to serotonin at the onset of starvation, animals were deposited directly onto serotonin plates after food removal. To expose animals to serotonin after 3 hours of starvation, animals were starved for 3 hours on standard starvation plates then were transferred to serotonin plates via washing in M9 + 0.01% Tween-20.

cdk-1 RNAi

RNAi was performed by feeding. A *cdk-1* RNAi clone and the empty RNAi vector (L440) were obtained from the Ahringer library (Kamath and Ahringer, 2003) and grown overnight at 37˚C in liquid Luria Broth + 60 µg/ml carbenicillin + 10 µg/ml tetracycline. Cells were concentrated 5-fold, then spotted onto plates containing nematode growth media supplemented with 60 µg/ml carbenicillin, 10 µg/ml tetracycline, and 1 mM IPTG. Plates were spotted one day before adding worms.

Temperature shifts

Temperature shifts were performed by transferring plates of worms from 15˚C to 25˚C or the reverse. To expedite equilibration of plates to the new temperature, plates were buried in a

single layer within a 5-x-7-x-13 inch box full of unseeded plates pre-equilibrated at the new temperature.

For temperature shifts of fed *glp-1(q224ts)* animals, fed early adult hermaphrodites were shifted to 25˚C. Gonads were dissected every 30-60 minutes after the shift (for Figure 5H) or after 8 hours (for Figure 5A,I). Alternately, animals were maintained at 25˚C for 8 hours, then returned to 15˚C for 2-3 days (for Figure 5A).

For temperature shifts of *cdk-1* RNAi-treated animals (Figure 5B and Figure 5—figure supplement 1), *glp-1(q224ts)* animals were grown at 15˚C (on OP50) to mid L4, then transferred to *cdk-1* RNAi plates or L440 plates for 42 hours. Plates were then shifted to 25˚C for 8 hours, then returned to 15˚C for 2-3 days. At the beginning of the temperature shift, animals were adults, and germ cells in the progenitor zone had uniformly arrested in interphase, as evidenced by the absence of mitotic figures. Some nuclei in the progenitor zone had slightly enlarged, characteristic of *cdk-1*(RNAi)-induced cell-cycle arrest (Jeong et al., 2011). Nuclear morphology was otherwise normal (Figure 5—figure supplement 1).

For temperature shifts of starved *glp-1(q224ts)* animals, hermaphrodites were starved at 15˚C from early adult for 2-4 hours or from mid L4 for 24 hours. For Figure 5C-D, starved animals were shifted to 25˚C for 8, 16, or 24 hours, returned to 15˚C for 8-12 hours, then re-fed at 15˚C for 2-3 days. At the beginning of the temperature shift, animals starved from L4 were adults. For Figure 5G-H, animals were shifted to 25˚C for 8 hours, then re-fed at 25˚C. For Figure 5I, animals were shifted to 25˚C for 8 hours.

For temperature shifts of *glp-1(q224ts)* animals exposed to high NaCl (Figure 5E), early adult hermaphrodites were transferred to plates containing high NaCl media and incubated at 15˚C for 2 hours. Animals were then shifted to 25˚C for 8 hours, returned to 15˚C for 12 hours, then transferred to plates containing standard media for 2-3 days. High NaCl media was identical to standard media, except that it contained a total of 17.4 g/L (300 mM) NaCl.

For temperature shifts of (unmated) *fog-1(q785); glp-1(q224ts)* animals (Figure 5F), hermaphrodites aged 40 hours post mid L4 were shifted to 25˚C for 8 hours, then returned to 15˚C for 2-3 days. Animals aged 40-hours post mid L4 were used because the reduced mitotic index caused by absence of sperm is not fully evident at the early adult stage (40-hours post mid L4 at 15˚C is roughly equivalent to 24-hours post mid-L4 at 20˚C). For temperature shifts of mated *fog-1(q785); glp-1(q224ts)* animals, *fog-1(q785); glp-1(q224ts)* mid L4 hermaphrodites

were transferred to plates with CB4856 males in a ratio of 1:2. After 40 hours of mating, hermaphrodites wearing copulatory plugs were transferred to fresh plates (at 15˚C), then shifted to 25˚C for 8 hours.

Temperature shifts of *emb-30(tn377ts)* animals are described below.

***emb-30(tn377ts)* experiments and analyses**

emb-30(tn377ts) animals were grown at 15˚C to mid L4, then starved at 15˚C for 24 hours, by which time animals were adults. Animals were then shifted to 25˚C for 14 hours and either re-fed or maintained in starvation. Gonads were dissected immediately before re-feeding and at one-hour intervals 2-6 hours after re-feeding. Gonads were also dissected after 6 hours of continued starvation. Gonads were stained for phospho-histone H3 and GLD-1 and imaged at 63X magnification with a z-stack interval of 1 μm. Cells were identified using IRISES (Vogel et al., 2014), followed by manual correction using the Cell Counter plug-in in Image J. Cells were classified as interphase, M-phase, or 'crescent' (i.e. meiotic prophase) according to chromosome morphology and phosopho-histone H3 staining. Occasionally, at the later re-feeding timepoints, cells were observed bypassing the metaphase arrest; for the purposes of this experiment, such cells were classified as M-phase. Cells distal to the 'crescent'/'non-crescent' boundary were defined as cells whose midpoints were located distal to a cross-sectional line drawn through the midpoint of the second most distal 'crescent' cell. Relative positions of cells along the distal-to-proximal axis were determined by collapsing cell positions along the z-axis and fitting these positions to a second-degree polynomial curve. Positions along this polynomial curve closest to each germ cell and closest to the distal tip cell we identified (by solving, for each cell, the polynomial whose roots minimize this distance). Using this new set of positions, distances between the distal tip cell and each germ cell were calculated. Cells were then ranked according to these distances.

Sample sizes

In experiments requiring image acquisition, an attempt was made to examine at least 20 gonads. In other experiments, an attempt was made to examine at least 50 gonads.

Plots

Plots were generated in part using the ggplot package for R (ggplot2.org).

Acknowledgements

We thank Jadwiga Forster for media preparation, Peggy Kroll-Conner for worm maintenance, and Sarah Crittenden, Kim Haupt, Aaron Kershner, and Erika Sorensen for comments on the manuscript. Some strains were provided by the *Caenorhabditis* Genetics Center, which is funded by National Institutes of Health Office of Research Infrastructure Programs (P40 OD010440). JK is an investigator of the Howard Hughes Medical Institute. HSS was supported by an Ellison Medical Foundation Fellowship of the Life Science Research Foundation.

Competing interests

The authors declare no competing interests.

Figure 1. Fed versus starved adult hermaphrodite gonads of *C. elegans*. (A) Schematic of an adult hermaphrodite gonadal arm, with the progenitor zone at its distal end and maturing gametes at its proximal end. Germline stem cells and transient progenitors are located in the distal and proximal progenitor zone, respectively. Cells in both pools cycle asynchronously, although they are partially connected via a cytoplasmic core. Filled circles, germ cell nuclei in the progenitor zone. Open circles, germ cell nuclei in meiotic prophase, including developing oocytes. Gonads in males and larval hermaphrodites are organized similarly, although their proximal germ cells differentiate as sperm. This same gonad organization is also seen in starved animals of any stage or sex for time intervals examined in this work. (B) Images of distal gonads dissected from adult hermaphrodites and stained with DAPI to visualize DNA (magenta) and anti-phospho-histone H3 to visualize M-phase chromosomes (green). M-phase cells are outlined and numbered. Left, fed early adult hermaphrodite. Right, hermaphrodite starved from early adult for 8 hours. (See Materials and methods for definition of 'early adult'.) Asterisks, distal gonad ends. Images are maximum-intensity z-projections.

Figure 2. Mitotic divisions in adult progenitor zones respond quickly to food removal and re-feeding. Timecourses showing the number M-phase cells per progenitor zone after food removal or re-feeding. Time zero indicates the start of food removal or re-feeding. Animals in A-B and D-E were starved from early adult. Animals in C were starved from mid L4. Animals in F were starved from mid L4 for 24 hours or from early L4 for 72 hours. Independent replicates are over-plotted with transparency. For each replicate, lines connect means, and shaded areas show interquartile ranges. Sample sizes indicate numbers of gonadal arms. Source data are available in Figure 2—source data 1.

Figure 2—figure supplement 1. Comparison of numbers of M-phase cells in fed, starved, and re-fed animals. (A-D) Timecourses showing the number M-phase cells per progenitor zone in adult hermaphrodites exposed to food removal, mock food removal, or continuous feeding. For food removal or mock food removal, time zero indicates start of food removal or mock food removal. For continuous feeding, time zero indicates the time at which animals reached the early adult stage or the '24-hour post mid L4' stage. (E-F) Normalized histograms showing the number of M-phase cells per progenitor zone for fed or re-fed adults. Data for fed animals are reproduced from the 'before food removal' timepoints of Figure 2A and C. Data for re-fed animals are reproduced from Figure 2B and D. Source data are available in Figure 2—source data 1.

Figure 3. Starvation slows S phase and causes germ cells to arrest in G2. (A) Timecourses showing the proportion of progenitor-zone cells in G1, S phase, or G2, for animals starved from early adult or from mid or early L4. Animals starved from mid L4 were adults at the 10.5- and 24-hour timepoints. Animals starved from early L4 were adults at the 24-, 48-, and 72-hours timepoints. n = 19-40 gonadal arms per timepoint. (B) Timecourses showing the number of cells in the progenitor zone, for the same gonads used in A. Within each plot, lines connect means, and shaded areas show interquartile ranges. (C) Schematic summarizing the effect of starvation on the mitotic cell cycle of germ cells. Cell-cycle length under fed conditions was measured in adult hermaphrodites (Figure 3—figure supplement 1). Source data are available in Figure 3—source data 1.

Figure 3—figure supplement 1. Measurements of cell-cycle length in fed animals. (A) Proportions of progenitor-zone cells in each phase of the cell cycle in fed early adult hermaphrodites and fed adult hermaphrodites aged 24-hours post mid L4 ('L4 + 24 h'). Data for early adults derives from the 'before food removal' timepoint of the timecourse in Figure 3A. Data for L4 + 24 animals derives from 0.5-hour timepoint of the timecourse in C. Sample sizes indicate number of gonadal arms. (B) Number of progenitor-zone cells for the same gonads used in C. (C) EdU-labeling timecourse to measure G2 length. Fed early adult hermaphrodites and hermaphrodites aged 24-hours post mid L4 were exposed to continuous EdU labeling. The proportion of M-phase cells that were EdU^+ was measured at the timepoints shown. Open green circle, sample contained some gonadal arms in which all progenitor-zone cells were EdU^+. Filled green circle, all progenitor-zone cells in all gonadal arms were EdU^+ cells. (D) Median indices for each cell-cycle phase, calculated from the data in A. (E) Time at which 50%, 95%, or 100% of M-phase cells were EdU^+, from the timecourse in C. (F) Median length of each cell-cycle phase and the total cell cycle, calculated from the data in D-E. (G) Estimates of maximum total cell-cycle length, calculated from the data in E-F. Source data for A-B are available in Figure 3—source data 2. Source data for C are available in Figure 3—source data 3.

Figure 3—figure supplement 2. G1 versus G2 cells can be distinguished by nuclear size in EdU-labeled gonads. (A) Propidium iodide intensities (a measure of DNA content) versus nuclear volume for interphase progenitor-zone nuclei and the distal tip cell nucleus in six gonadal arms. Propidium iodide intensities are scaled relative to the distal tip cell and the mean of G2 cells, to account for gonad-to-gonad differences in staining. Left, fed early adult hermaphrodites. Right, hermaphrodites starved from early adult for 3.5 hours. Cell-cycle phases were assigned by EdU uptake (S-phase cells) and nuclear size (G1 versus G2). AU, arbitrary units. (B) Images of EdU-labeled distal gonads (15 min EdU pulse) dissected from fed early adult hermaphrodites and stained with DAPI to visualize DNA (magenta). Asterisks, distal gonad ends. Dashed lines, progenitor zone boundaries. Yellow and blue circles, examples of G1 and G2 nuclei, respectively. Caret, paired occurrence of G1 cells. (C) Images of progenitor-zone nuclei in each stage of the cell cycle. Nuclei derive from gonads described as in B. Source data are available in Figure 3—source data 3.

Figure 4. Ectopic mitotic divisions outside the progenitor zone respond normally to food removal and re-feeding. Timecourses showing the number of M-phase cells—outside the distal-most 20 rows of germ cells—after food removal or re-feeding in adult *glp-1(oz112gf)* hermaphrodites or adult *gld-3(q730) nos-3(q650)* hermaphrodites. Time zero indicates the start of food removal or re-feeding. Lines connect means, and shaded areas show interquartile ranges. n = 50-249 gonadal arms per timepoint. Source data are available in Figure 4—source data 1.

Figure 5. Quiescence induced by three different conditions maintains germline stem cells independent of GLP-1/Notch. (A-F) Distance between the gonad distal tip and the first 'crescent' germ cell for adult hermaphrodites of the genotypes and treatments shown. Animals were grown at 15˚, shifted to 25˚ for 8, 16, or 24 hours, then returned to 15˚ for 2-3 days. Gonads were collected prior to the temperature shift (15˚), immediately following the temperature shift (25˚ 8h, 25˚ 16h, or 25˚ 24h), and following the 15˚ recovery period (… + 15˚ 2-3d). Data are plotted as vertical histograms, with black circles denoting means. n = 55-488 gonadal arms per timepoint. (G) Timecourse showing the number of M-phase cells per progenitor zone in *glp-1(q224ts)* hermaphrodites starved from early adult, shifted to 25˚ for 8 hours, then re-fed at 25˚. Lines connect means, and shaded areas show interquartile ranges. (H) Timecourses showing distance between the gonad distal tip and the first 'crescent' germ cell. Top, hermaphrodites starved from early adult, shifted to 25˚ for 8 hours, then re-fed at 25˚. Bottom, hermaphrodites fed continuously and shifted to 25˚ at the early adult stage. Data are plotted as vertical histograms, with lines connecting means. Sample sizes in G-H indicate number of gonadal arms. (I) Images of distal gonads dissected from adult hermaphrodites and stained with DAPI to visualize DNA (magenta) and anti-GLD-1 (green). Gonads were dissected before and after 8 hours at 25˚. Left-hand panels, fed adult hermaphrodites. Right-hand panels, hermaphrodites starved from early adult. Asterisks, distal gonad ends. (J) Schematic summarizing the effect of cell-cycle quiescence on germline stem cell maintenance. Under conditions of active proliferation, GLP-1/Notch is required for germline stem cell maintenance. Under quiescent conditions, GLP-1/Notch is dispensable. Source data for A-F are available in Figure 5—source data 1. Source data for G-H are available in Figure 5—source data 2.

Figure 5—figure supplement 1. Cell-cycle arrest caused by *cdk-1* RNAi does not maintain germline stem cells in absence of GLP-1/Notch. Images of distal gonads dissected from *glp-1(q224ts)* adult hermaphrodites exposed to *cdk-1* RNAi (lower panels) or the empty RNAi vector, L440 (upper panels). Gonads were dissected before and after 8 hours at 25˚ and stained with DAPI to visualize DNA (magenta) and anti-HIM-3 (green) to visualize formation of the synaptonymal complex, indicating meiotic entry (Zetka et al., 1999). Asterisks, distal gonad ends. Arrowheads, examples of nuclei in the distal ends in which HIM-3 has been loaded onto chromosomes. Dashed lines, progenitor zone boundaries. Images are maximum-intensity z-projections.

Figure 6. Re-feeding restores the rate of progression through S phase and G2, as well as the meiotic entry of transient progenitors. (A) Images of distal gonads dissected from *emb-30(tn377ts)* adult hermaphrodites and stained with DAPI to visualize DNA (magenta) and anti-GLD-1 (green). Animals were starved at 15˚, shifted to 25˚, then either re-fed or maintained in starvation. Time = 0 h indicates the time at which re-feeding was started or starvation continued. Top, starved adult hermaphrodite, Time = 0 h. Middle, re-fed adult hermaphrodite, Time = 6 h. Bottom, adult hermaphrodite maintained in starvation, Time = 6 h. Dashed lines, 'crescent'/'non-crescent' boundaries (defined by the second distal-most 'crescent' cell—see Materials and methods). Arrowhead, example of a metaphase-arrested cell having a high level of GLD-1. Asterisks, distal gonad ends. Images are maximum-intensity z-projections. (B) Timecourse showing the proportion of cells in M-phase (among the distal-most 50 germ cells) for *emb-30(tn377ts)* adult hermaphrodites treated as in A. n = 31-66 gonadal arms per timepoint. (C) Number of cells distal to the 'crescent'/'non-crescent' boundary for the same gonads used in B. (D) Cell-cycle behavior, among cells distal to the 'crescent'/'non-crescent' boundary, for the same gonads used in B. Cells from individual gonadal arms are plotted along lines, with color indicating cell-cycle phase (interphase or M-phase) and location determined by each cell's position along the distal-to-proximal axis of distal gonad. For each timepoint, this axis is scaled relative to the mean number of cells distal to the 'crescent'/'non-crescent' boundary. (E) Summary of the effects of re-feeding and continued starvation on germ cells in *emb-30(tn377ts)* hermaphrodites in the distal versus proximal progenitor zone. (F) Summary of the effects of starvation on germ cell division, stem cell maintenance, and meiotic entry. Under fed conditions, mitotic cell divisions occur throughout the progenitor zone (Crittenden et al., 2006; Maciejowski et al., 2006); GLP-1/Notch is required for stem cell maintenance (Austin and Kimble, 1987); and transient progenitors enter the meiotic cell cycle if their movement out of the progenitor zone is restricted (Cinquin et al., 2010). Under starved conditions, germ cells become quiescent; GLP-1/Notch is dispensable for stem cell maintenance; and the meiotic entry of transient progenitors is slowed or blocked. Source data are available in Figure 6—source data 1.

Figure 7. Starvation-induced quiescence is distinct from the DNA damage response and does not require factors involved in larval or behavioral responses to food. (A) Images of distal gonads dissected from adult hermaphrodites and stained with DAPI to visualize DNA (magenta) and anti-phosopho-CDK-1 (green, Santa Cruz #sc-28435-R) to visualize inhibitory phosphorylation of CDK-1. The phospho-specificity of anti-phosopho-CDK-1 is shown in Figure 7—figure supplement 1. Top row, fed adult hermaphrodite. Center row, adult hermaphrodite starved from early adult for 8 hours. Bottom row, fed adult hermaphrodite treated with UV light to induce DNA damage. Asterisks, distal gonad ends. Arrowheads, example of an enlarged nucleus having elevated phospho-CDK-1. Similar results were observed using a different phospho-CDK-1 antibody (Calbiochem #219440, data not shown). (B) Timecourses showing the mean number of M-phase cells per progenitor zone after food removal for hermaphrodites of the genotypes shown. Animals were starved from early adult. Grey curves represent seven replicates of wildtype, reproduced from Figure 2A. Time zero indicates the start of food removal. Lower right corner, wildtype hermaphrodites exposed to 20 mM serotonin at the onset of food removal (0 hours) or 3 hours later. n = 46-452 gonadal arms per timepoint. Source data are available in Figure 7—source data 1.

Figure 7—figure supplement 1. Validation of phospho-specificity of anti-phosopho-CDK-1. Images of whole gonadal arms dissected from fed early adult hermaphrodites. Gonads were treated with or without lambda protein phosphatase and stained with anti-phosopho-CDK-1 (Santa Cruz #sc-28435-R) and DAPI to visualize DNA. Images are maximum-intensity z-projections.

Figure 2—source data 1. Counts of M-phase cells for starvation and re-feeding timecourses of wildtype animals. This comma-separated value file contains counts of M-phase cells per gonadal arm for starvation, re-feeding, and control timecourses of wildtype animals (Figure 2 and Figure 2—figure supplement 1). Each row of the file represents a single gonadal arm. Descriptors include treatment group (starvation, re-feeding, mock starvation, continued feeding), animal sex (hermaphrodite, male), age at the start of treatment (L4, early adult, L4 + 24h), replicate, and time.

Figure 3—source data 1. Counts of cells in each phase of the cell cycle for starvation timecourses of wildtype animals. This comma-separated value file contains counts of progenitor-zone cells in each phase of the cell cycle for starvation timecourses of wildtype animals (Figure 3). Each row of the file represents a single cell. Descriptors include cell-cycle phase (G1, S-phase, G2, M-phase), animal sex (hermaphrodite, male), age at the start of starvation (early L4, mid L4, early adult), time, and a gonad identifier.

Figure 3—source data 2. Counts of cells in each phase of the cell cycle for fed adult wildtype hermaphrodites. This comma-separated value file contains counts of progenitor-zone cells in each phase of the cell cycle for fed early adult hermaphrodites and fed hermaphrodites aged 24 hours post mid L4 (Figure 3—figure supplement 1A-B). Each set of four rows of the file represents a single progenitor zone. Descriptors include cell-cycle phase (G1, S-phase, G2, M-phase), age (early adult, L4 + 24h), and a gonad identifier.

Figure 3—source data 3. EdU labeling in fed adult wildtype hermaphrodites. This comma-separated value file contains counts of EdU-positive and EdU-negative M-phase cells in hermaphrodites exposed to EdU from the early adult stage or from 24 hours post mid L4 (Figure 3—figure supplement 1C). Each rows of the file represents a single timepoint. Descriptors indicate age at the start of EdU labeling (early adult, L4 + 24h).

Figure 3—source data 4. Propidium iodide intensities versus nuclear volume in the progenitor-zone. This comma-separated value file contains propidium iodide intensities and nuclear volumes of interphase progenitor-zone nuclei and distal tip cell nuclei of six EdU-labeled gonadal arms (Figure 3—figure supplement 2). Gonadal arms are from fed early adult hermaphrodites or hermaphrodites starved from early adult for 3.5 hours. Each row of the file represents a single cell. Descriptors include treatment group (fed, starved), cell-cycle phase (G1, S-phase, G2, distal tip cell), and a gonad identifier.

Figure 4—source data 1. Counts of M-phase cells for starvation and re-feeding timecourses of *glp-1(oz112gf)* and *gld-3(q730) nos-3(q650)* hermaphrodites. This comma-separated value file contains counts of M-phase cells per gonadal arm for *glp-1(oz112gf)* and *gld-3(q730) nos-3(q650)* starvation and re-feeding timecourses (Figure 4). Each row of the file represents a single gonadal arm. Descriptors include treatment group (starvation, re-feeding), genotype (*glp-1(oz112gf)*, *gld-3(q730) nos-3(q650)*), and time.

Figure 5—source data 1. Temperature-shift experiments of *glp-1(q224)* hermaphrodites. This comma-separated value file contains measurements of the distance between the gonad distal tip and the first 'crescent' germ cell in temperature-shifted *glp-1(q224)* hermaphrodites (Figure 5A-F). Distances are measured in germ cell diameters. Each row of the file represents a single gonadal arm. Descriptors include growth conditions (fed, *cdk-1* RNAi, starved from early adult, starved from mid-L4, 300 mM NaCl, no sperm) and temperature (15˚; 25˚ 8h; 25˚ 16h; 25˚ 24h; 25˚ 8h + 15˚ 2-3d; 25˚ 16h + 15˚ 2-3d; 25˚ 24h + 15˚ 2-3d).

Figure 5—source data 2. Timecourses of temperature-shifted *glp-1(q224)* hermaphrodites. This comma-separated value file contains counts of M-phase cells and distances between the gonad distal tip and the first 'crescent' germ cell for two groups of animals: (i) *glp-1(q224ts)* hermaphrodites starved from early adult, shifted to 25˚ for 8 hours, then re-fed at 25˚, and (ii) *glp-1(q224ts)* hermaphrodites fed continuously and shifted to 25˚ at the early adult stage (Figure 5G-H). Distances are measured in germ cell diameters. Each row of the file represents a single gonadal arm. Descriptors include treatment group (fed, starved) and time. NA, not determined.

Figure 6—source data 1. Temperature-shift experiments of *emb-30(tn377ts)* hermaphrodites. This comma-separated value file contains counts of interphase and M-phase progenitor-zone cells for *emb-30(tn377ts)* hermaphrodites re-fed at the restrictive temperature or maintained in continued starvation (Figure 6). Each row of the file represents a single cell. Descriptors include treatment group (re-fed, starved), cell-cycle phase (interphase, M-phase), ranked proximity to the distal tip cell (numeric), time, and a gonad identifier.

Figure 7—source data 1. Starvation timecourses of mutants and of wildtype hermaphrodites exposed to exogenous serotonin. This comma-separated value file contains counts of M-phase cells per gonadal arm for the starvation timecourses shown in Figure 7B. Each row of the file represents a single gonadal arm. Descriptors include genotype (*cep-1(gk138), aak-2(gt33)*, …) and time. For serotonin exposure, genotype is listed as 'serotonin 0h' or 'serotonin 3h'.

References

Adesanya, O.O., J. Zhou, C. Samathanam, L. Powell-Braxton, and C.A. Bondy. 1999. Insulin-like growth factor 1 is required for G2 progression in the estradiol-induced mitotic cycle. *Proc Natl Acad Sci U S A*. 96:3287-3291.

Agathocleous, M., and W.A. Harris. 2013. Metabolism in physiological cell proliferation and differentiation. *Trends Cell Biol*. 23:484-492.

Aldewachi, H.S., N.A. Wright, D.R. Appleton, and A.J. Watson. 1975. The effect of starvation and refeeding on cell population kinetics in the rat small bowel mucosa. *J Anat*. 119:105-121.

Angelo, G., and M.R. Van Gilst. 2009. Starvation protects germline stem cells and extends reproductive longevity in C. elegans. *Science*. 326:954-958.

Armstrong, A.R., K.M. Laws, and D. Drummond-Barbosa. 2014. Adipocyte amino acid sensing controls adult germline stem cell number via the amino acid response pathway and independently of Target of Rapamycin signaling in Drosophila. *Development*. 141:4479-4488.

Asselin-Labat, M.L., F. Vaillant, J.M. Sheridan, B. Pal, D. Wu, E.R. Simpson, H. Yasuda, G.K. Smyth, T.J. Martin, G.J. Lindeman, and J.E. Visvader. 2010. Control of mammary stem cell function by steroid hormone signalling. *Nature*. 465:798-802.

Austin, J., and J. Kimble. 1987. glp-1 is required in the germ line for regulation of the decision between mitosis and meiosis in C. elegans. *Cell*. 51:589-599.

Barker, N., S. Bartfeld, and H. Clevers. 2010a. Tissue-resident adult stem cell populations of rapidly self-renewing organs. *Cell Stem Cell*. 7:656-670.

Barker, N., M. Huch, P. Kujala, M. van de Wetering, H.J. Snippert, J.H. van Es, T. Sato, D.E. Stange, H. Begthel, M. van den Born, E. Danenberg, S. van den Brink, J. Korving, A. Abo, P.J. Peters, N. Wright, R. Poulsom, and H. Clevers. 2010b. Lgr5(+ve) stem cells drive self-renewal in the stomach and build long-lived gastric units in vitro. *Cell Stem Cell*. 6:25-36.

Bergtold, W.H. 1926. Avian Gonads and Migration. *The Condor*. 28:114-120.

1066 Berry, L.W., B. Westlund, and T. Schedl. 1997. Germ-line tumor formation caused by activation
1067 of glp-1, a Caenorhabditis elegans member of the Notch family of receptors.
1068 *Development*. 124:925-936.

1069 Blacque, O.E., M.J. Reardon, C. Li, J. McCarthy, M.R. Mahjoub, S.J. Ansley, J.L. Badano, A.K.
1070 Mah, P.L. Beales, W.S. Davidson, R.C. Johnsen, M. Audeh, R.H. Plasterk, D.L. Baillie,
1071 N. Katsanis, L.M. Quarmby, S.R. Wicks, and M.R. Leroux. 2004. Loss of C. elegans
1072 BBS-7 and BBS-8 protein function results in cilia defects and compromised intraflagellar
1073 transport. *Genes Dev*. 18:1630-1642.

1074 Bonfini, A., M.B. Wilkin, and M. Baron. 2015. Reversible regulation of stem cell niche size
1075 associated with dietary control of Notch signalling. *BMC Dev Biol*. 15:8.

1076 Bouldin, C.M., and D. Kimelman. 2014. Cdc25 and the importance of G2 control: insights from
1077 developmental biology. *Cell Cycle*. 13:2165-2171.

1078 Bouldin, C.M., C.D. Snelson, G.H. Farr, 3rd, and D. Kimelman. 2014. Restricted expression of
1079 cdc25a in the tailbud is essential for formation of the zebrafish posterior body. *Genes*
1080 *Dev*. 28:384-395.

1081 Butuci, M., A.B. Williams, M.M. Wong, B. Kramer, and W.M. Michael. 2015. Zygotic Genome
1082 Activation Triggers Chromosome Damage and Checkpoint Signaling in C. elegans
1083 Primordial Germ Cells. *Dev Cell*. 34:85-95.

1084 Byrd, D.T., K. Knobel, K. Affeldt, S.L. Crittenden, and J. Kimble. 2014. A DTC niche plexus
1085 surrounds the germline stem cell pool in Caenorhabditis elegans. *PLoS One*. 9:e88372.

1086 Cameron, I.L., and N.C. Bols. 1975. Effect of cell population density on G2 arrest in
1087 Tetrahymena. *J Cell Biol*. 67:518-522.

1088 Cameron, I.L., and G. Cleffmann. 1964. Initiation of mitosis in relation to the cell cycle
1089 following feeding of starved chickens. *J Cell Biol*. 21:169-174.

1090 Chen, N., A. Mah, O.E. Blacque, J. Chu, K. Phgora, M.W. Bakhoum, C.R. Newbury, J. Khattra,
1091 S. Chan, A. Go, E. Efimenko, R. Johnsen, P. Phirke, P. Swoboda, M. Marra, D.G.
1092 Moerman, M.R. Leroux, D.L. Baillie, and L.D. Stein. 2006. Identification of ciliary and
1093 ciliopathy genes in Caenorhabditis elegans through comparative genomics. *Genome Biol*.
1094 7:R126.

1095 Cheung, T.H., and T.A. Rando. 2013. Molecular regulation of stem cell quiescence. *Nat Rev Mol*
1096 *Cell Biol*. 14:329-340.

1097 Chiang, M., A. Cinquin, A. Paz, E. Meeds, C.A. Price, M. Welling, and O. Cinquin. 2015.
1098 Control of C. elegans germline stem cell cycling speed meets requirements of design to
1099 minimize mutation accumulation. *BMC Biol*. 13:51.

1100 Cinquin, O., S.L. Crittenden, D.E. Morgan, and J. Kimble. 2010. Progression from a stem cell-
1101 like state to early differentiation in the C. elegans germ line. *Proc Natl Acad Sci U S A*.
1102 107:2048-2053.

1103 Consortium, C.e.D.M. 2012. large-scale screening for targeted knockouts in the Caenorhabditis
1104 elegans genome. *G3 (Bethesda)*. 2:1415-1425.

1105 Costello, G., L. Rodgers, and D. Beach. 1986. Fission yeast enters the stationary phase G0 state
1106 from either mitotic G1 or G2. *Curr Genet*. 11:119-125.

1107 Craig, A.L., S.C. Moser, A.P. Bailly, and A. Gartner. 2012. Methods for studying the DNA
1108 damage response in the Caenorhabdatis elegans germ line. *Methods Cell Biol*. 107:321-
1109 352.

1110 Crittenden, S.L., D.S. Bernstein, J.L. Bachorik, B.E. Thompson, M. Gallegos, A.G. Petcherski,
1111 G. Moulder, R. Barstead, M. Wickens, and J. Kimble. 2002. A conserved RNA-binding
1112 protein controls germline stem cells in Caenorhabditis elegans. *Nature*. 417:660-663.

1113 Crittenden, S.L., K.A. Leonhard, D.T. Byrd, and J. Kimble. 2006. Cellular analyses of the
1114 mitotic region in the Caenorhabditis elegans adult germ line. *Mol Biol Cell*. 17:3051-
1115 3061.

1116 da Graca, L.S., K.K. Zimmerman, M.C. Mitchell, M. Kozhan-Gorodetska, K. Sekiewicz, Y.
1117 Morales, and G.I. Patterson. 2004. DAF-5 is a Ski oncoprotein homolog that functions in
1118 a neuronal TGF beta pathway to regulate C. elegans dauer development. *Development*.
1119 131:435-446.

1120 Dalfo, D., D. Michaelson, and E.J. Hubbard. 2012. Sensory regulation of the C. elegans germline
1121 through TGF-beta-dependent signaling in the niche. *Curr Biol*. 22:712-719.

1122 de Navascues, J., C.N. Perdigoto, Y. Bian, M.H. Schneider, A.J. Bardin, A. Martinez-Arias, and
1123 B.D. Simons. 2012. Drosophila midgut homeostasis involves neutral competition
1124 between symmetrically dividing intestinal stem cells. *EMBO J*. 31:2473-2485.

1125 Dernburg, A.F., K. McDonald, G. Moulder, R. Barstead, M. Dresser, and A.M. Villeneuve.
1126 1998. Meiotic recombination in C. elegans initiates by a conserved mechanism and is
1127 dispensable for homologous chromosome synapsis. *Cell*. 94:387-398.

1128 Derry, W.B., R. Bierings, M. van Iersel, T. Satkunendran, V. Reinke, and J.H. Rothman. 2007.
1129 Regulation of developmental rate and germ cell proliferation in Caenorhabditis elegans
1130 by the p53 gene network. *Cell Death Differ*. 14:662-670.

1131 Doetsch, F., I. Caille, D.A. Lim, J.M. Garcia-Verdugo, and A. Alvarez-Buylla. 1999.
1132 Subventricular zone astrocytes are neural stem cells in the adult mammalian brain. *Cell*.
1133 97:703-716.

1134 Doupe, D.P., and P.H. Jones. 2013. Cycling progenitors maintain epithelia while diverse cell
1135 types contribute to repair. *Bioessays*. 35:443-451.

1136 Drummond-Barbosa, D., and A.C. Spradling. 2001. Stem cells and their progeny respond to
1137 nutritional changes during Drosophila oogenesis. *Dev Biol*. 231:265-278.

1138 Eckmann, C.R., S.L. Crittenden, N. Suh, and J. Kimble. 2004. GLD-3 and control of the
1139 mitosis/meiosis decision in the germline of Caenorhabditis elegans. *Genetics*. 168:147-
1140 160.

1141 Fox, P.M., and T. Schedl. 2015. Analysis of Germline Stem Cell Differentiation Following Loss
1142 of GLP-1 Notch Activity in Caenorhabditis elegans. *Genetics*.

1143 Fox, P.M., V.E. Vought, M. Hanazawa, M.H. Lee, E.M. Maine, and T. Schedl. 2011. Cyclin E
1144 and CDK-2 regulate proliferative cell fate and cell cycle progression in the C. elegans
1145 germline. *Development*. 138:2223-2234.

1146 Frederick, T.J., and T.L. Wood. 2004. IGF-I and FGF-2 coordinately enhance cyclin D1 and
1147 cyclin E-cdk2 association and activity to promote G1 progression in oligodendrocyte
1148 progenitor cells. *Mol Cell Neurosci*. 25:480-492.

1149 Fuchs, E. 2009. The tortoise and the hair: slow-cycling cells in the stem cell race. *Cell*. 137:811-
1150 819.

1151 Fukuyama, M., A.E. Rougvie, and J.H. Rothman. 2006. C. elegans DAF-18/PTEN mediates
1152 nutrient-dependent arrest of cell cycle and growth in the germline. *Curr Biol*. 16:773-779.

1153 Fukuyama, M., K. Sakuma, R. Park, H. Kasuga, R. Nagaya, Y. Atsumi, Y. Shimomura, S.
1154 Takahashi, H. Kajiho, A. Rougvie, K. Kontani, and T. Katada. 2012. C. elegans AMPKs
1155 promote survival and arrest germline development during nutrient stress. *Biol Open*.
1156 1:929-936.

1157 Furuta, T., S. Tuck, J. Kirchner, B. Koch, R. Auty, R. Kitagawa, A.M. Rose, and D. Greenstein.
1158 2000. EMB-30: an APC4 homologue required for metaphase-to-anaphase transitions
1159 during meiosis and mitosis in Caenorhabditis elegans. *Mol Biol Cell*. 11:1401-1419.

1160 Gartner, A., S. Milstein, S. Ahmed, J. Hodgkin, and M.O. Hengartner. 2000. A conserved
1161 checkpoint pathway mediates DNA damage--induced apoptosis and cell cycle arrest in C.
1162 elegans. *Mol Cell*. 5:435-443.

1163 Gelfant, S. 1977. A new concept of tissue and tumor cell proliferation. *Cancer Res*. 37:3845-
1164 3862.

1165 Gerhold, A.R., J. Ryan, J.N. Vallee-Trudeau, J.F. Dorn, J.C. Labbe, and P.S. Maddox. 2015.
1166 Investigating the regulation of stem and progenitor cell mitotic progression by in situ
1167 imaging. *Curr Biol*. 25:1123-1134.

1168 Gracheva, E.O., A.O. Burdina, A.M. Holgado, M. Berthelot-Grosjean, B.D. Ackley, G.
1169 Hadwiger, M.L. Nonet, R.M. Weimer, and J.E. Richmond. 2006. Tomosyn inhibits
1170 synaptic vesicle priming in Caenorhabditis elegans. *PLoS Biol*. 4:e261.

1171 Hachet, V., C. Canard, and P. Gonczy. 2007. Centrosomes promote timely mitotic entry in C.
1172 elegans embryos. *Dev Cell*. 12:531-541.

1173 Hagemann, R.F., and J.J. Stragand. 1977. Fasting and refeeding: cell kinetic response of
1174 jejunum, ileum and colon. *Cell Tissue Kinet*. 10:3-14.

1175 Hall, P.A., and F.M. Watt. 1989. Stem cells: the generation and maintenance of cellular
1176 diversity. *Development*. 106:619-633.

1177 Hans, F., and S. Dimitrov. 2001. Histone H3 phosphorylation and cell division. *Oncogene*.
1178 20:3021-3027.

1179 Harrison, D.E., and C.P. Lerner. 1991. Most primitive hematopoietic stem cells are stimulated to
1180 cycle rapidly after treatment with 5-fluorouracil. *Blood*. 78:1237-1240.

1181 Hartman, T.R., T.I. Strochlic, Y. Ji, D. Zinshteyn, and A.M. O'Reilly. 2013. Diet controls
1182 Drosophila follicle stem cell proliferation via Hedgehog sequestration and release. *J Cell*
1183 *Biol*. 201:741-757.

1184 Henderson, S.T., D. Gao, E.J. Lambie, and J. Kimble. 1994. lag-2 may encode a signaling ligand
1185 for the GLP-1 and LIN-12 receptors of C. elegans. *Development*. 120:2913-2924.

1186 Hodgkin, J., and T. Doniach. 1997. Natural variation and copulatory plug formation in
1187 Caenorhabditis elegans. *Genetics*. 146:149-164.

1188 Hsu, H.J., and D. Drummond-Barbosa. 2011. Insulin signals control the competence of the
1189 Drosophila female germline stem cell niche to respond to Notch ligands. *Dev Biol*.
1190 350:290-300.

1191 Hsu, H.J., L. LaFever, and D. Drummond-Barbosa. 2008. Diet controls normal and tumorous
1192 germline stem cells via insulin-dependent and -independent mechanisms in Drosophila.
1193 *Dev Biol*. 313:700-712.

1194 Husson, S.J., E. Clynen, G. Baggerman, T. Janssen, and L. Schoofs. 2006. Defective processing
1195 of neuropeptide precursors in Caenorhabditis elegans lacking proprotein convertase 2
1196 (KPC-2/EGL-3): mutant analysis by mass spectrometry. *J Neurochem*. 98:1999-2012.

1197 Husson, S.J., T. Janssen, G. Baggerman, B. Bogert, A.H. Kahn-Kirby, K. Ashrafi, and L.
1198 Schoofs. 2007. Impaired processing of FLP and NLP peptides in carboxypeptidase E
1199 (EGL-21)-deficient Caenorhabditis elegans as analyzed by mass spectrometry. *J*
1200 *Neurochem*. 102:246-260.

1201 Jaramillo-Lambert, A., M. Ellefson, A.M. Villeneuve, and J. Engebrecht. 2007. Differential
1202 timing of S phases, X chromosome replication, and meiotic prophase in the C. elegans
1203 germ line. *Dev Biol*. 308:206-221.

1204 Jeong, J., J.M. Verheyden, and J. Kimble. 2011. Cyclin E and Cdk2 control GLD-1, the
1205 mitosis/meiosis decision, and germline stem cells in Caenorhabditis elegans. *PLoS Genet*.
1206 7:e1001348.

1207 Jones, A.R., R. Francis, and T. Schedl. 1996. GLD-1, a cytoplasmic protein essential for oocyte
1208 differentiation, shows stage- and sex-specific expression during Caenorhabditis elegans
1209 germline development. *Dev Biol*. 180:165-183.

1210 Joshi, P.A., H.W. Jackson, A.G. Beristain, M.A. Di Grappa, P.A. Mote, C.L. Clarke, J. Stingl,
1211 P.D. Waterhouse, and R. Khokha. 2010. Progesterone induces adult mammary stem cell
1212 expansion. *Nature*. 465:803-807.

1213 Jouandin, P., C. Ghiglione, and S. Noselli. 2014. Starvation induces FoxO-dependent mitotic-to-
1214 endocycle switch pausing during Drosophila oogenesis. *Development*. 141:3013-3021.

1215 Kamath, R.S., and J. Ahringer. 2003. Genome-wide RNAi screening in Caenorhabditis elegans.
1216 *Methods*. 30:313-321.

1217 Kershner, A.M., H. Shin, T.J. Hansen, and J. Kimble. 2014. Discovery of two GLP-1/Notch
1218 target genes that account for the role of GLP-1/Notch signaling in stem cell maintenance.
1219 *Proc Natl Acad Sci U S A*. 111:3739-3744.

1220 Kimble, J., and S.L. Crittenden. 2007. Controls of germline stem cells, entry into meiosis, and
1221 the sperm/oocyte decision in Caenorhabditis elegans. *Annu Rev Cell Dev Biol*. 23:405-
1222 433.

1223 Kimble, J., and H.S. Seidel. 2013. C. elegans germline stem cells and their niche. *In* StemBook.
1224 T.S.C.R. Community, editor. StemBook.

1225 Kodoyianni, V., E.M. Maine, and J. Kimble. 1992. Molecular basis of loss-of-function mutations
1226 in the glp-1 gene of Caenorhabditis elegans. *Mol Biol Cell*. 3:1199-1213.

1227 Korta, D.Z., S. Tuck, and E.J. Hubbard. 2012. S6K links cell fate, cell cycle and nutrient
1228 response in C. elegans germline stem/progenitor cells. *Development*. 139:859-870.

1229 Kruman, II, E.N. Ilyasova, S.A. Rudchenko, and Z.S. Khurkhulu. 1988. The intestinal epithelial
1230 cells of ground squirrel (Citellus undulatus) accumulate at G2 phase of the cell cycle
1231 throughout a bout of hibernation. *Comp Biochem Physiol A Comp Physiol*. 90:233-236.

1232 Kuntz, K., and M.J. O'Connell. 2009. The G(2) DNA damage checkpoint: could this ancient
1233 regulator be the Achilles heel of cancer? *Cancer Biol Ther*. 8:1433-1439.

1234 LaFever, L., A. Feoktistov, H.J. Hsu, and D. Drummond-Barbosa. 2010. Specific roles of Target
1235 of rapamycin in the control of stem cells and their progeny in the Drosophila ovary.
1236 *Development*. 137:2117-2126.

1237 Laporte, D., A. Lebaudy, A. Sahin, B. Pinson, J. Ceschin, B. Daignan-Fornier, and I. Sagot.
1238 2011. Metabolic status rather than cell cycle signals control quiescence entry and exit. *J*
1239 *Cell Biol*. 192:949-957.

1240 Lascarez-Lagunas, L.I., C.G. Silva-Garcia, T.D. Dinkova, and R.E. Navarro. 2014. LIN-35/Rb
1241 causes starvation-induced germ cell apoptosis via CED-9/Bcl2 downregulation in
1242 Caenorhabditis elegans. *Mol Cell Biol*. 34:2499-2516.

1243 Lawrence, K.S., T. Chau, and J. Engebrecht. 2015. DNA Damage Response and Spindle
1244 Assembly Checkpoint Function throughout the Cell Cycle to Ensure Genomic Integrity.
1245 *PLoS Genet*. 11:e1005150.

1246 Lee, B.H., J. Liu, D. Wong, S. Srinivasan, and K. Ashrafi. 2011. Hyperactive neuroendocrine
1247 secretion causes size, feeding, and metabolic defects of C. elegans Bardet-Biedl
1248 syndrome mutants. *PLoS Biol*. 9:e1001219.

1249 Lee, H., J.S. Cho, N. Lambacher, J. Lee, S.J. Lee, T.H. Lee, A. Gartner, and H.S. Koo. 2008. The
1250 Caenorhabditis elegans AMP-activated protein kinase AAK-2 is phosphorylated by
1251 LKB1 and is required for resistance to oxidative stress and for normal motility and
1252 foraging behavior. *J Biol Chem*. 283:14988-14993.

1253 Lin, K., J.B. Dorman, A. Rodan, and C. Kenyon. 1997. daf-16: An HNF-3/forkhead family
1254 member that can function to double the life-span of Caenorhabditis elegans. *Science*.
1255 278:1319-1322.

1256 Lopez, A.L., 3rd, J. Chen, H.J. Joo, M. Drake, M. Shidate, C. Kseib, and S. Arur. 2013. DAF-2
1257 and ERK couple nutrient availability to meiotic progression during Caenorhabditis
1258 elegans oogenesis. *Dev Cell*. 27:227-240.

1259 Love, N.K., N. Keshavan, R. Lewis, W.A. Harris, and M. Agathocleous. 2014. A nutrient-
1260 sensitive restriction point is active during retinal progenitor cell differentiation.
1261 *Development*. 141:697-706.

1262 Luedtke, S., V. O'Connor, L. Holden-Dye, and R.J. Walker. 2010. The regulation of feeding and
1263 metabolism in response to food deprivation in Caenorhabditis elegans. *Invert Neurosci*.
1264 10:63-76.

1265 Lugert, S., O. Basak, P. Knuckles, U. Haussler, K. Fabel, M. Gotz, C.A. Haas, G. Kempermann,
1266 V. Taylor, and C. Giachino. 2010. Quiescent and active hippocampal neural stem cells
1267 with distinct morphologies respond selectively to physiological and pathological stimuli
1268 and aging. *Cell Stem Cell*. 6:445-456.

1269 Lum, J.J., D.E. Bauer, M. Kong, M.H. Harris, C. Li, T. Lindsten, and C.B. Thompson. 2005.
1270 Growth factor regulation of autophagy and cell survival in the absence of apoptosis. *Cell*.
1271 120:237-248.

1272 Maciejowski, J., N. Ugel, B. Mishra, M. Isopi, and E.J. Hubbard. 2006. Quantitative analysis of
1273 germline mitosis in adult C. elegans. *Dev Biol*. 292:142-151.

McLeod, C.J., L. Wang, C. Wong, and D.L. Jones. 2010. Stem cell dynamics in response to nutrient availability. *Curr Biol*. 20:2100-2105.

Michaelson, D., D.Z. Korta, Y. Capua, and E.J. Hubbard. 2010. Insulin signaling promotes germline proliferation in C. elegans. *Development*. 137:671-680.

Mihaylova, V.T., C.Z. Borland, L. Manjarrez, M.J. Stern, and H. Sun. 1999. The PTEN tumor suppressor homolog in Caenorhabditis elegans regulates longevity and dauer formation in an insulin receptor-like signaling pathway. *Proc Natl Acad Sci U S A*. 96:7427-7432.

Min, J., S. Singh, P. Fitzgerald-Bocarsly, and T.L. Wood. 2012. Insulin-like growth factor I regulates G2/M progression through mammalian target of rapamycin signaling in oligodendrocyte progenitors. *Glia*. 60:1684-1695.

Morgan, D.E., S.L. Crittenden, and J. Kimble. 2010. The C. elegans adult male germline: stem cells and sexual dimorphism. *Dev Biol*. 346:204-214.

Morris, L.X., and A.C. Spradling. 2011. Long-term live imaging provides new insight into stem cell regulation and germline-soma coordination in the Drosophila ovary. *Development*. 138:2207-2215.

Nadarajan, S., J.A. Govindan, M. McGovern, E.J. Hubbard, and D. Greenstein. 2009. MSP and GLP-1/Notch signaling coordinately regulate actomyosin-dependent cytoplasmic streaming and oocyte growth in C. elegans. *Development*. 136:2223-2234.

Narbonne, P., and R. Roy. 2006. Inhibition of germline proliferation during C. elegans dauer development requires PTEN, LKB1 and AMPK signalling. *Development*. 133:611-619.

O'Brien, L.E., S.S. Soliman, X. Li, and D. Bilder. 2011. Altered modes of stem cell division drive adaptive intestinal growth. *Cell*. 147:603-614.

Orford, K.W., and D.T. Scadden. 2008. Deconstructing stem cell self-renewal: genetic insights into cell-cycle regulation. *Nat Rev Genet*. 9:115-128.

Paradis, S., and G. Ruvkun. 1998. Caenorhabditis elegans Akt/PKB transduces insulin receptor-like signals from AGE-1 PI3 kinase to the DAF-16 transcription factor. *Genes Dev*. 12:2488-2498.

Pardee, A.B. 1974. A restriction point for control of normal animal cell proliferation. *Proc Natl Acad Sci U S A*. 71:1286-1290.

Pardee, A.B. 1989. G1 events and regulation of cell proliferation. *Science*. 246:603-608.

Patterson, G.I., A. Koweek, A. Wong, Y. Liu, and G. Ruvkun. 1997. The DAF-3 Smad protein antagonizes TGF-beta-related receptor signaling in the Caenorhabditis elegans dauer pathway. *Genes Dev*. 11:2679-2690.

1307 Perens, E.A., and S. Shaham. 2005. C. elegans daf-6 encodes a patched-related protein required
1308 for lumen formation. *Dev Cell*. 8:893-906.

1309 Pietras, E.M., M.R. Warr, and E. Passegue. 2011. Cell cycle regulation in hematopoietic stem
1310 cells. *J Cell Biol*. 195:709-720.

1311 Potten, C.S., and M. Loeffler. 1990. Stem cells: attributes, cycles, spirals, pitfalls and
1312 uncertainties. Lessons for and from the crypt. *Development*. 110:1001-1020.

1313 Qiao, X.T., J.W. Ziel, W. McKimpson, B.B. Madison, A. Todisco, J.L. Merchant, L.C.
1314 Samuelson, and D.L. Gumucio. 2007. Prospective identification of a multilineage
1315 progenitor in murine stomach epithelium. *Gastroenterology*. 133:1989-1998.

1316 Rahman, M.M., S. Rosu, D. Joseph-Strauss, and O. Cohen-Fix. 2014. Down-regulation of
1317 tricarboxylic acid (TCA) cycle genes blocks progression through the first mitotic division
1318 in Caenorhabditis elegans embryos. *Proc Natl Acad Sci U S A*. 111:2602-2607.

1319 Rieder, C.L. 2011. Mitosis in vertebrates: the G2/M and M/A transitions and their associated
1320 checkpoints. *Chromosome Res*. 19:291-306.

1321 Roth, T.M., C.Y. Chiang, M. Inaba, H. Yuan, V. Salzmann, C.E. Roth, and Y.M. Yamashita.
1322 2012. Centrosome misorientation mediates slowing of the cell cycle under limited
1323 nutrient conditions in Drosophila male germline stem cells. *Mol Biol Cell*. 23:1524-1532.

1324 Salinas, L.S., E. Maldonado, and R.E. Navarro. 2006. Stress-induced germ cell apoptosis by a
1325 p53 independent pathway in Caenorhabditis elegans. *Cell Death Differ*. 13:2129-2139.

1326 Secor, S.M., and J. Diamond. 1998. A vertebrate model of extreme physiological regulation.
1327 *Nature*. 395:659-662.

1328 Seidel, H.S., and J. Kimble. 2011. The oogenic germline starvation response in C. elegans. *PLoS*
1329 *One*. 6:e28074.

1330 Sheng, X.R., and E. Matunis. 2011. Live imaging of the Drosophila spermatogonial stem cell
1331 niche reveals novel mechanisms regulating germline stem cell output. *Development*.
1332 138:3367-3376.

1333 Sieburth, D., J.M. Madison, and J.M. Kaplan. 2007. PKC-1 regulates secretion of neuropeptides.
1334 *Nat Neurosci*. 10:49-57.

1335 Simons, B.D., and H. Clevers. 2011. Strategies for homeostatic stem cell self-renewal in adult
1336 tissues. *Cell*. 145:851-862.

1337 Snippert, H.J., L.G. van der Flier, T. Sato, J.H. van Es, M. van den Born, C. Kroon-Veenboer, N.
1338 Barker, A.M. Klein, J. van Rheenen, B.D. Simons, and H. Clevers. 2010. Intestinal crypt
1339 homeostasis results from neutral competition between symmetrically dividing Lgr5 stem
1340 cells. *Cell*. 143:134-144.

1341 Soprano, K.J. 1994. WI-38 cell long-term quiescence model system: a valuable tool to study
1342 molecular events that regulate growth. *J Cell Biochem*. 54:405-414.

1343 Speese, S., M. Petrie, K. Schuske, M. Ailion, K. Ann, K. Iwasaki, E.M. Jorgensen, and T.F.
1344 Martin. 2007. UNC-31 (CAPS) is required for dense-core vesicle but not synaptic vesicle
1345 exocytosis in Caenorhabditis elegans. *J Neurosci*. 27:6150-6162.

1346 Spriggs, K.A., M. Bushell, and A.E. Willis. 2010. Translational regulation of gene expression
1347 during conditions of cell stress. *Mol Cell*. 40:228-237.

1348 Starich, T.A., D.H. Hall, and D. Greenstein. 2014. Two classes of gap junction channels mediate
1349 soma-germline interactions essential for germline proliferation and gametogenesis in
1350 Caenorhabditis elegans. *Genetics*. 198:1127-1153.

1351 Stromberg, T., S. Ekman, L. Girnita, L.Y. Dimberg, O. Larsson, M. Axelson, J. Lennartsson, U.
1352 Hellman, K. Carlson, A. Osterborg, K. Vanderkerken, K. Nilsson, and H. Jernberg-
1353 Wiklund. 2006. IGF-1 receptor tyrosine kinase inhibition by the cyclolignan PPP induces
1354 G2/M-phase accumulation and apoptosis in multiple myeloma cells. *Blood*. 107:669-678.

1355 Usai, K., and K. Kimura. 1992. Sensory mother cells are selected from among mitotically
1356 quiescent cluster of cells in the wing disc of Drosophila. *Development*. 116:601-610.

1357 Vogel, J.L., D. Michaelson, A. Santella, E.J. Hubbard, and Z. Bao. 2014. Irises: A practical tool
1358 for image-based analysis of cellular DNA content. *Worm*. 3:e29041.

1359 Wabik, A., and P.H. Jones. 2015. Switching roles: the functional plasticity of adult tissue stem
1360 cells. *EMBO J*. 34:1164-1179.

1361 Wang, S., X. Wang, Y. Wu, and C. Han. 2015. IGF-1R signaling is essential for the proliferation
1362 of cultured mouse spermatogonial stem cells by promoting the G2/M progression of the
1363 cell cycle. *Stem Cells Dev*. 24:471-483.

1364 Watts, J.L., D.G. Morton, J. Bestman, and K.J. Kemphues. 2000. The C. elegans par-4 gene
1365 encodes a putative serine-threonine kinase required for establishing embryonic
1366 asymmetry. *Development*. 127:1467-1475.

1367 Yang, H., and Y.M. Yamashita. 2015. The regulated elimination of transit-amplifying cells
1368 preserves tissue homeostasis during protein starvation in Drosophila testis. *Development*.
1369 142:1756-1766.

1370 Yilmaz, O.H., P. Katajisto, D.W. Lamming, Y. Gultekin, K.E. Bauer-Rowe, S. Sengupta, K.
1371 Birsoy, A. Dursun, V.O. Yilmaz, M. Selig, G.P. Nielsen, M. Mino-Kenudson, L.R.
1372 Zukerberg, A.K. Bhan, V. Deshpande, and D.M. Sabatini. 2012. mTORC1 in the Paneth
1373 cell niche couples intestinal stem-cell function to calorie intake. *Nature*. 486:490-495.

1374 Zetka, M.C., I. Kawasaki, S. Strome, and F. Muller. 1999. Synapsis and chiasma formation in
1375 Caenorhabditis elegans require HIM-3, a meiotic chromosome core component that
1376 functions in chromosome segregation. *Genes Dev*. 13:2258-2270.

1377 Zetterberg, A., and O. Larsson. 1985. Kinetic analysis of regulatory events in G1 leading to
1378 proliferation or quiescence of Swiss 3T3 cells. *Proc Natl Acad Sci U S A*. 82:5365-5369.

1379 Zielke, N., M. van Straaten, J. Bohlen, and B.A. Edgar. 2016. Using the Fly-FUCCI System for
1380 the Live Analysis of Cell Cycle Dynamics in Cultured Drosophila Cells. *Methods Mol*
1381 *Biol*. 1342:305-320.
1382

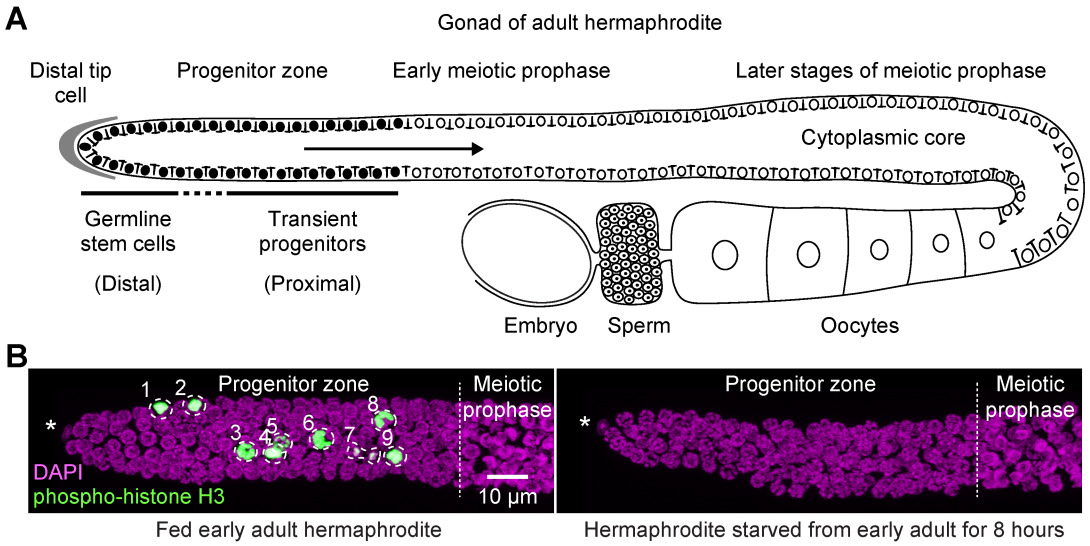
A
Gonad of adult hermaphrodite
Distal tip cell
Progenitor zone
Early meiotic prophase
Later stages of meiotic prophase
Cytoplasmic core
Germline stem cells
(Distal)
Transient progenitors
(Proximal)
Embryo
Sperm
Oocytes
B
Progenitor zone
Meiotic prophase
1
2
3
4
5
6
7
8
9
*
DAPI
phospho-histone H3
10 µm
Progenitor zone
Meiotic prophase
*
Fed early adult hermaphrodite
Hermaphrodite starved from early adult for 8 hours

Figure 1

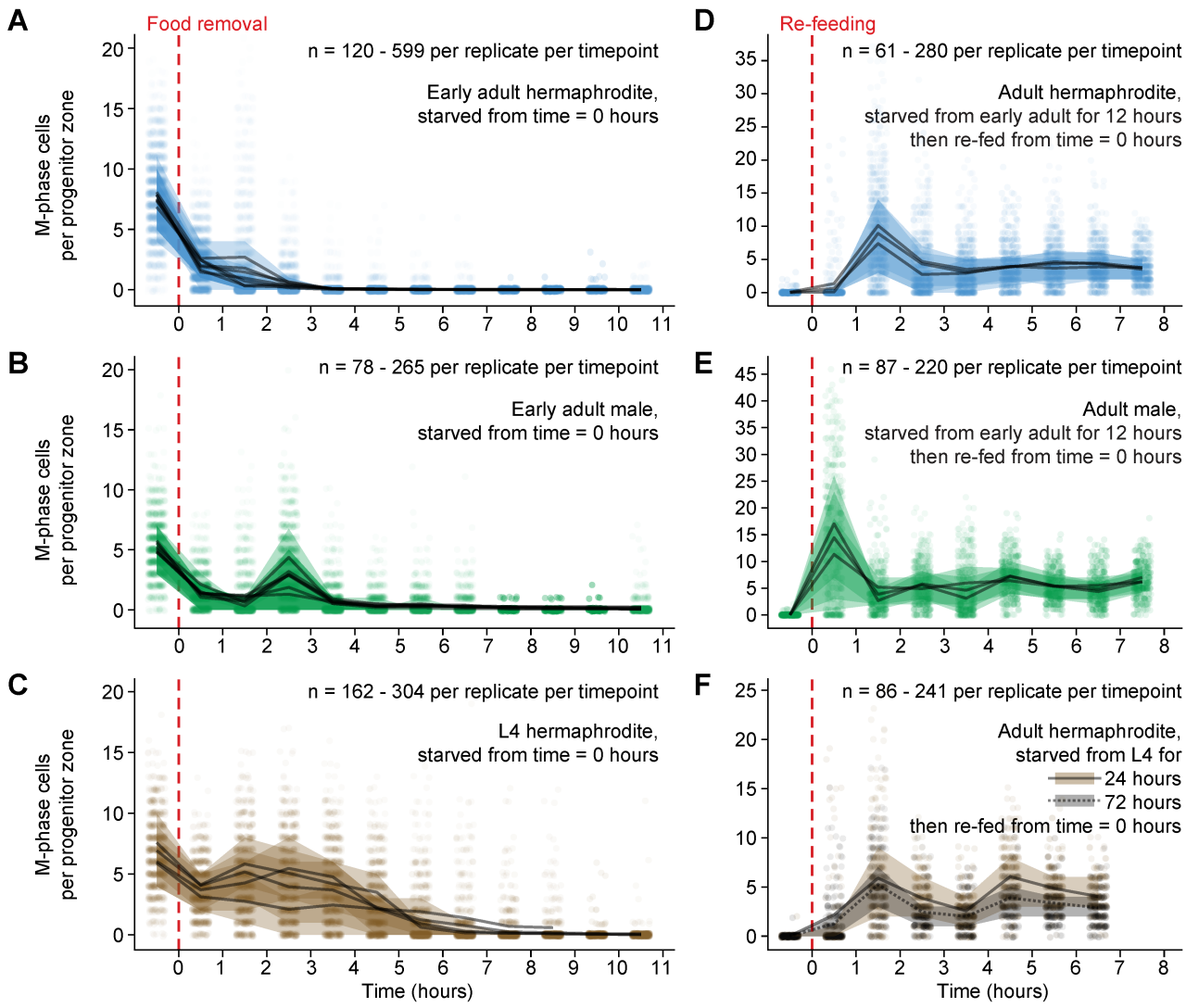
A
Food removal
n = 120 - 599 per replicate per timepoint
Early adult hermaphrodite,
starved from time = 0 hours
M-phase cells
per progenitor zone
B
n = 78 - 265 per replicate per timepoint
Early adult male,
starved from time = 0 hours
C
n = 162 - 304 per replicate per timepoint
L4 hermaphrodite,
starved from time = 0 hours
Time (hours)
D
Re-feeding
n = 61 - 280 per replicate per timepoint
Adult hermaphrodite,
starved from early adult for 12 hours
then re-fed from time = 0 hours
E
n = 87 - 220 per replicate per timepoint
Adult male,
starved from early adult for 12 hours
then re-fed from time = 0 hours
F
n = 86 - 241 per replicate per timepoint
Adult hermaphrodite,
starved from L4 for
24 hours
72 hours
then re-fed from time = 0 hours
Time (hours)

Figure 2

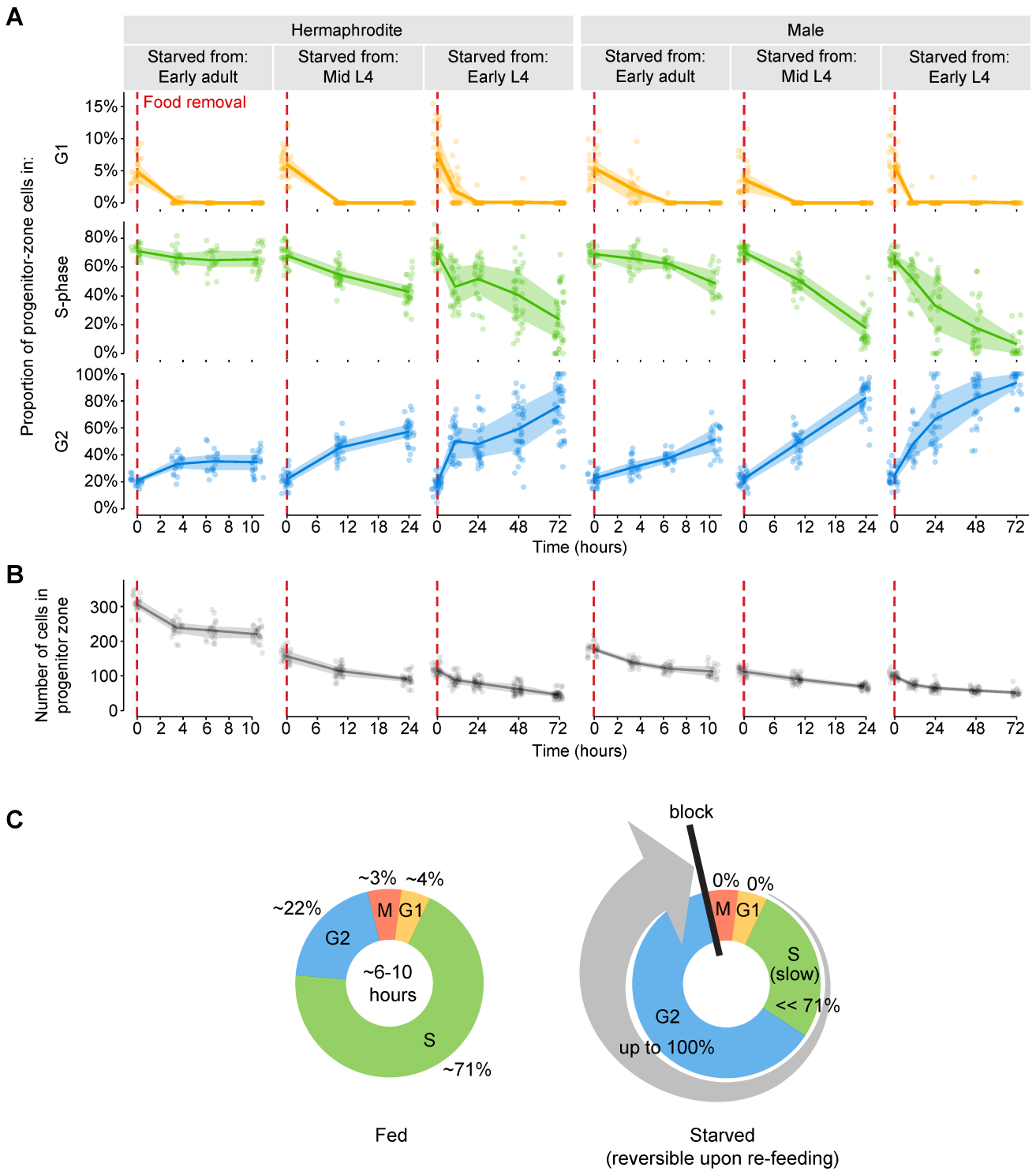
A
Hermaphrodite
Male
Starved from: Early adult
Starved from: Mid L4
Starved from: Early L4
Food removal
Proportion of progenitor-zone cells in:
G1
S-phase
G2
Time (hours)
B
Number of cells in progenitor zone
Time (hours)
C
~3%
~4%
~22%
M
G1
G2
~6-10 hours
S
~71%
Fed
block
0%
0%
M
G1
S (slow)
<< 71%
G2
up to 100%
Starved (reversible upon re-feeding)

Figure 3

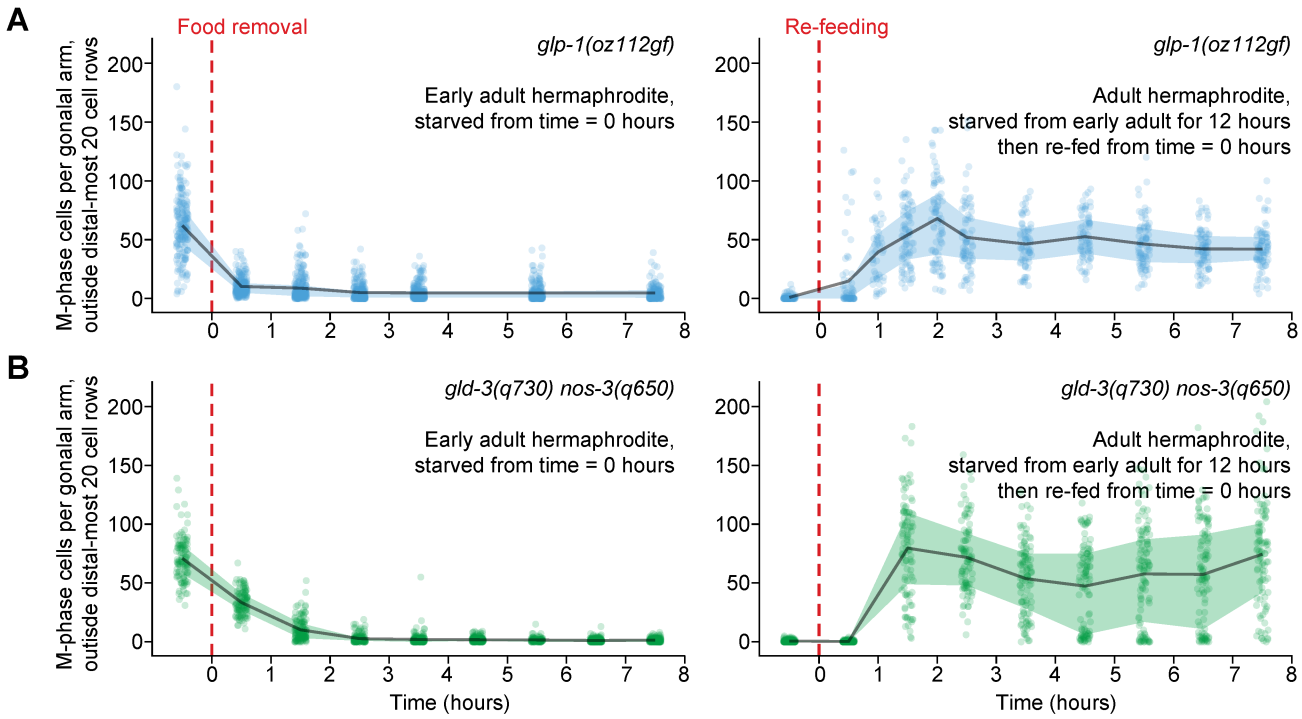
A
Food removal
glp-1(oz112gf)
Early adult hermaphrodite,
starved from time = 0 hours
Re-feeding
glp-1(oz112gf)
Adult hermaphrodite,
starved from early adult for 12 hours
then re-fed from time = 0 hours
B
gld-3(q730) nos-3(q650)
Early adult hermaphrodite,
starved from time = 0 hours
gld-3(q730) nos-3(q650)
Adult hermaphrodite,
starved from early adult for 12 hours
then re-fed from time = 0 hours
M-phase cells per gonalal arm,
outisde distal-most 20 cell rows
Time (hours)

Figure 4

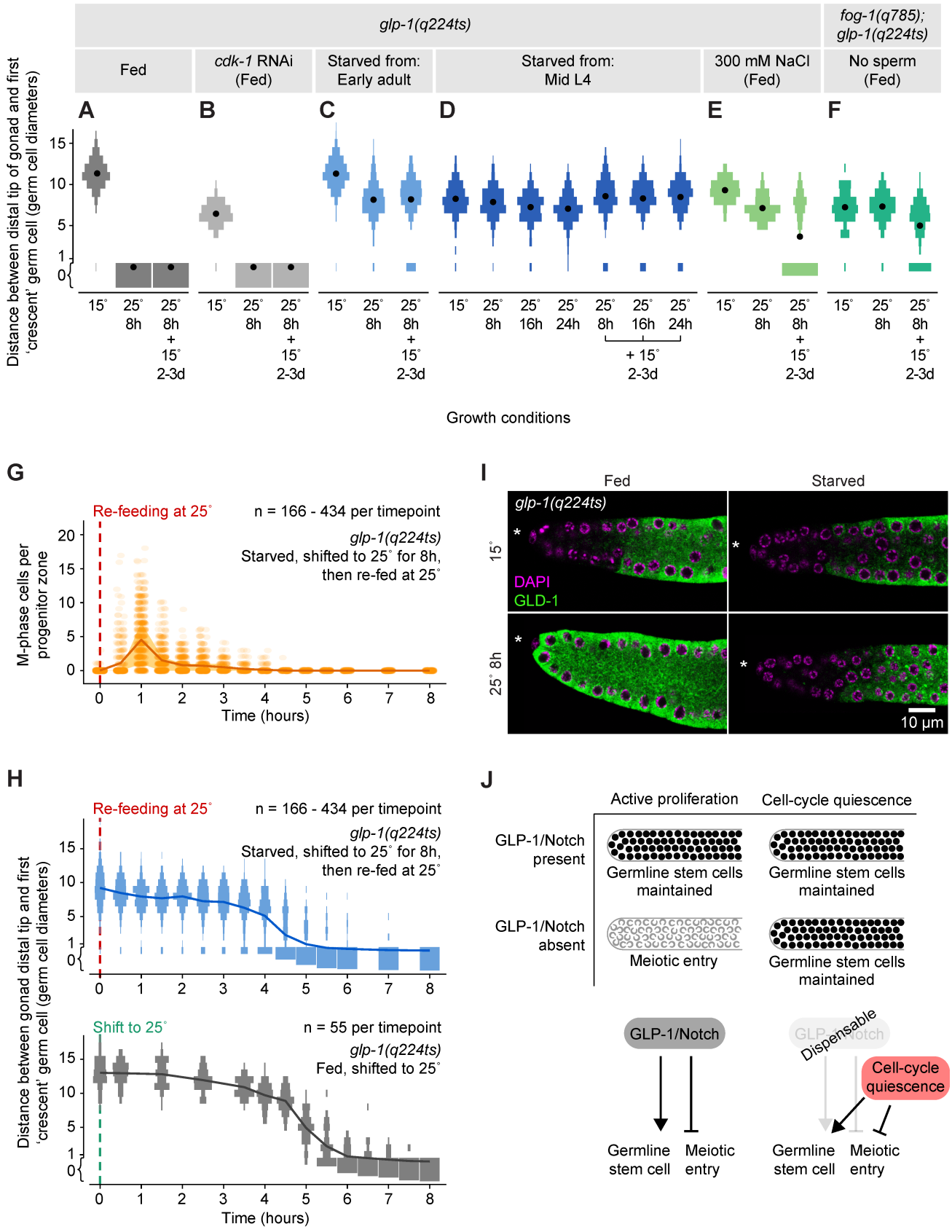
glp-1(q224ts)
fog-1(q785); glp-1(q224ts)
Fed
cdk-1 RNAi (Fed)
Starved from: Early adult
Starved from: Mid L4
300 mM NaCl (Fed)
No sperm (Fed)
A
B
C
D
E
F
Distance between distal tip of gonad and first 'crescent' germ cell (germ cell diameters)
15˚
25˚ 8h
25˚ 8h + 15˚ 2-3d
25˚ 16h
25˚ 24h
25˚ 8h + 15˚ 16h 24h + 15˚ 2-3d
Growth conditions
G
Re-feeding at 25˚
n = 166 - 434 per timepoint
glp-1(q224ts) Starved, shifted to 25˚ for 8h, then re-fed at 25˚
M-phase cells per progenitor zone
Time (hours)
H
Re-feeding at 25˚
n = 166 - 434 per timepoint
glp-1(q224ts) Starved, shifted to 25˚ for 8h, then re-fed at 25˚
Shift to 25˚
n = 55 per timepoint
glp-1(q224ts) Fed, shifted to 25˚
Distance between gonad distal tip and first 'crescent' germ cell (germ cell diameters)
Time (hours)
I
Fed
Starved
glp-1(q224ts)
15˚
25˚ 8h
DAPI
GLD-1
10 µm
J
Active proliferation
Cell-cycle quiescence
GLP-1/Notch present
GLP-1/Notch absent
Germline stem cells maintained
Meiotic entry
GLP-1/Notch
Dispensable
Cell-cycle quiescence
Germline stem cell
Meiotic entry

Figure 5

n = 31 - 66 per timepoint

n = 31 - 66 per timepoint

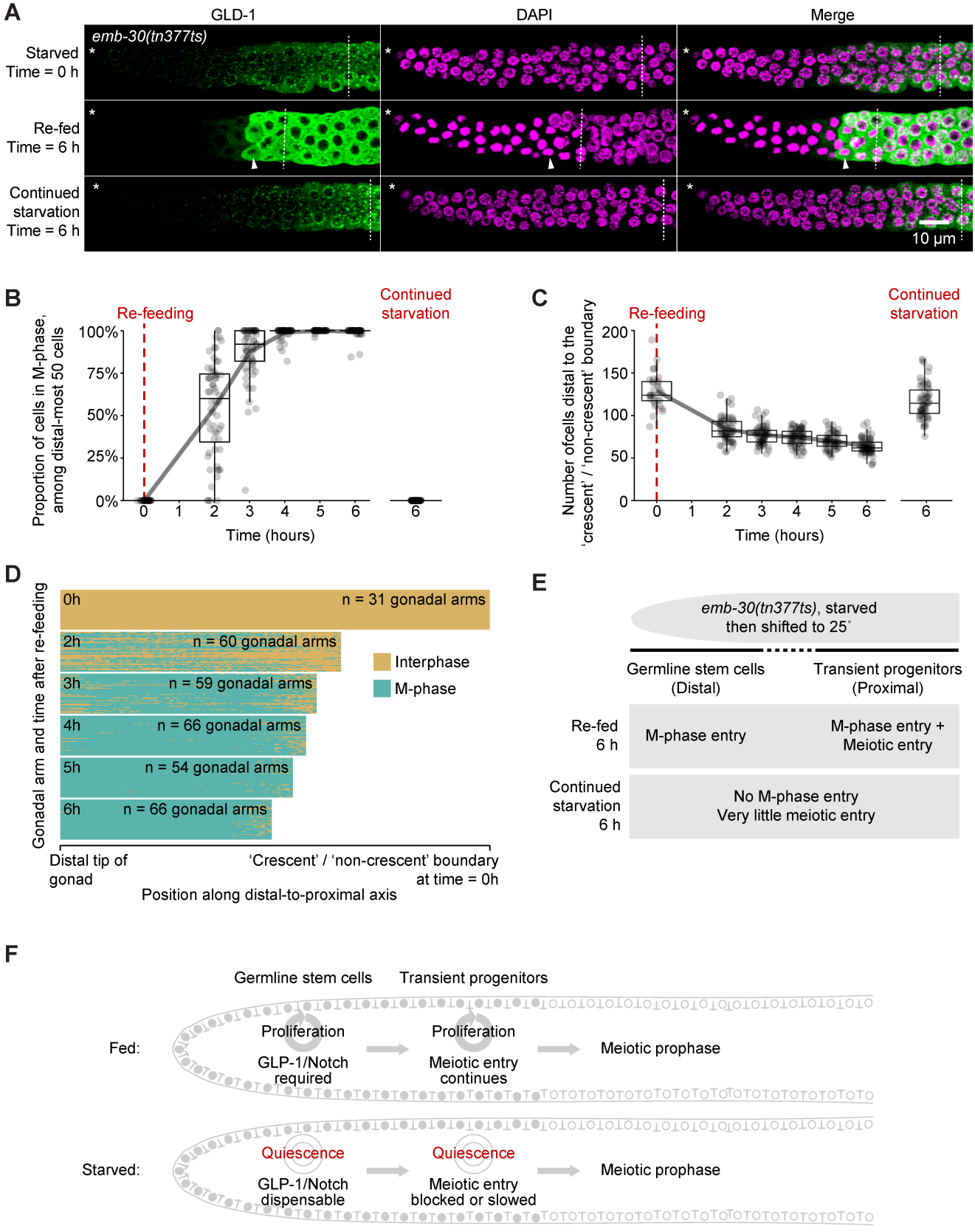

Figure 6

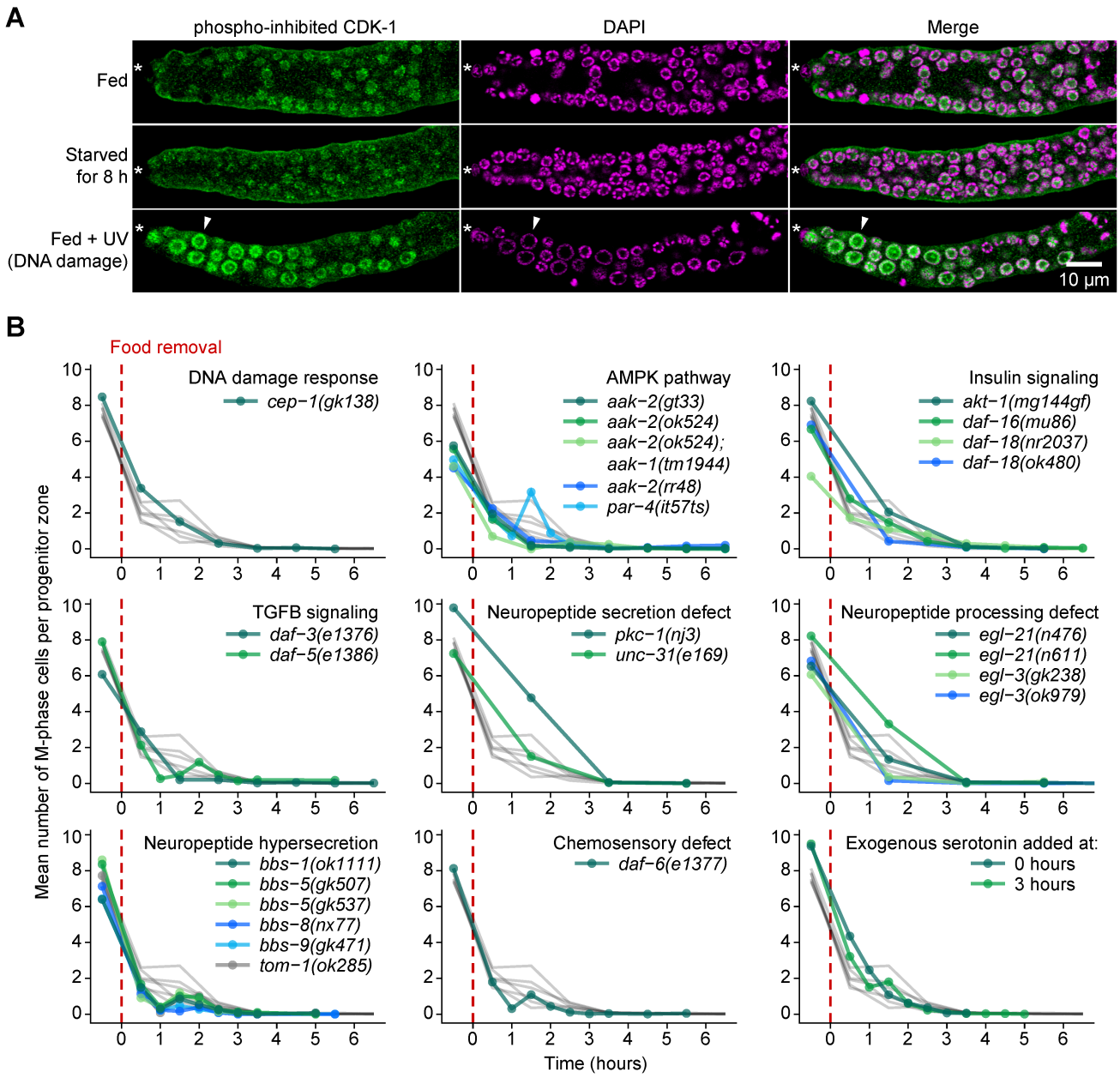
A
phospho-inhibited CDK-1
DAPI
Merge
Fed
Starved for 8 h
Fed + UV (DNA damage)
10 µm
B
Food removal
Mean number of M-phase cells per progenitor zone
Time (hours)
DNA damage response
cep−1(gk138)
AMPK pathway
aak−2(gt33)
aak−2(ok524)
aak−2(ok524); aak−1(tm1944)
aak−2(rr48)
par−4(it57ts)
Insulin signaling
akt−1(mg144gf)
daf−16(mu86)
daf−18(nr2037)
daf−18(ok480)
TGFB signaling
daf−3(e1376)
daf−5(e1386)
Neuropeptide secretion defect
pkc−1(nj3)
unc−31(e169)
Neuropeptide processing defect
egl−21(n476)
egl−21(n611)
egl−3(gk238)
egl−3(ok979)
Neuropeptide hypersecretion
bbs−1(ok1111)
bbs−5(gk507)
bbs−5(gk537)
bbs−8(nx77)
bbs−9(gk471)
tom−1(ok285)
Chemosensory defect
daf−6(e1377)
Exogenous serotonin added at:
0 hours
3 hours

Figure 7